1-1-2020

Determination Of The Gyro-Electric Reflection And Transmission Coefficients In The Fused Quartz Itop Cherenkov Particle Id Detectors At The Belle Ii Experiment

Michael Jeandron

DETERMINATION OF THE GYRO-ELECTRIC REFLECTION AND TRANSMISSION COEFFICIENTS IN THE FUSED QUARTZ ITOP CHERENKOV PARTICLE ID DETECTORS AT THE BELLE II EXPERIMENT

A Thesis
presented in partial fulfillment of requirements
for the degree of Master of Science
in the Department of Physics and Astronomy
The University of Mississippi

by

MICHAEL JEANDRON

May 2020

ABSTRACT

The thesis presents new results for the reflection and transmission coefficients for Cherenkov photons in a strong magnetic field at the interface between the fused quartz of and the surrounding nitrogen gas within the iTOP particle detector, a sub-system of the Belle II experiment. The iTOP is a component of the particle identification system at Belle II which distinguishes between kaons and pions in final states after collision. These coefficients are important in understanding how photons propagate through the iTOP taking into consideration polarization at the reflection and transmission interfaces in the Belle II magnetic field because the polarization affects the light collection efficiency of the detector.

A new coordinate system was employed which is valid for any face of the iTOP. Solutions for the electric and magnetic fields were found and verified using several wave equations that were derived from Maxwell's equations. Boundary conditions at the interface were written in the new coordinate system and solved to find the coefficients. These coefficients will be used in Monte Carlo simulations of photons propagating within the iTOP.

LIST OF ABBREVIATIONS AND SYMBOLS

CKM	Cabibbo-Kobayashi-Maskawa matrix
V	Verdet constant
B	Magnetic flux density
d	Distance traveled
n	Index of refraction
c	Speed of light in vacuum
v	Speed of light in a medium
iTOP	Imaging Time of Propagation detector
KEK	Kō Enerugī Kasokuki Kenkyū Kikō (High Energy Accelerator Research Organization)
CP	Charge-Parity
MC-PMT	Micro-Channel Photomultiplier tube
D	Electric displacement field
ϵ	Permittivity
E	Electric field
ω	Angular frequency
ω_L	Larmor frequency
t	Time
k	Wave vector
μ	Permeability
H	Magnetic field strength
TE	Transverse electric
TM	Transverse magnetic

α	Ratio of off diagonal to on diagonal elements of the permittivity tensor
r_+	Reflection coefficient
t_+	Transmission coefficient

ACKNOWLEDGEMENTS

I would like to thank my advisor, Dr. Robert Kroeger, and all of the professors who have contributed to my education with their continued support. I would also like to thank the Department of Physics and Astronomy for the many opportunities in teaching. Thanks to the U. S. Department of Energy, Office of Science.

TABLE OF CONTENTS

LIST OF FIGURES

CHAPTER 1

HISTORICAL CONTEXT OF THE FARADAY EFFECT

Michael Faraday, pictured in Figure 1, was born in 1791 in South London to James Faraday, a blacksmith's apprentice. The third of four children in a lower class family, Michael for the most part was forced to educate himself. At the age of 14, he took an apprenticeship with a local bookseller where he got the opportunity to read many books and develop an interest in science. At the end of his apprenticeship, Faraday started to attend chemistry lectures by Humphry Davy and soon became his assistant. During his work with Davy, he discovered two new compounds of chlorine and carbon, invented an early form of the Bunsen burner, and discovered the law of electrolysis. Throughout the 1820s and 30s, he began to experiment with electromagnetism which eventually led to his discovery of the law of induction. Even before his work, it was known that the polarization of light could be changed by certain materials. Because Faraday maintained that light was fundamentally electromagnetic in nature, he started to experiment with the effects a magnetic field might have on light as it passed through different objects. In 1845, he observed the rotation of the polarization of light due to the presence of a magnetic field. In his journal, he noted "[W]hen the contrary magnetic poles were on the same side, there was an effect produced on the polarized ray, and thus magnetic force and light were proved to have relation to each other." This phenomenon is now called the Faraday effect, and it shows that the angle of rotation is proportional to the strength of the magnetic field and the distance traveled through the object. Namely,

$$\theta = VBd \tag{1}$$

where θ is the angular rotation of the polarization, B is the magnetic field, d is the distance traveled, and the proportionality constant V is the Verdet constant. A more complicated expression must be used when the direction of propagation does not coincide with the direction of the B field. We refer to this general theory of propagation as the generalized Faraday rotation. It is described in detail in Belle Note 39 [1] and for Corning 7980 fused quartz glass, the rate of rotation, as determined by our measurements described in this Belle Note, is given by

$$\frac{d\theta}{dz} = B\left(-0.6786 - 0.8119\frac{e}{2mc}\lambda\frac{dn}{d\lambda}\right) cos\theta_B \tag{2}$$

where θ_B is the angle between the magnetic field and the direction of propagation, the units are rad/m, and the field is in Tesla.

Figure 1: Michael Faraday

CHAPTER 2

CHERENKOV RADIATION

First detected in 1934, Cherenkov radiation, as shown in Figure 2, is a process by which charged particles moving through a medium can give off photons [2]. Normally, particles are limited by the speed of light in vacuum, c. However, within a medium, the phase velocity of light, v, changes depending on the index of refraction, n, of the medium, given by $n = \frac{c}{v}$. Since the speed of light is lowered by media of a higher index, it is possible for a particle to enter a medium traveling faster than the phase velocity of light in that medium. When this occurs, photons on a wave front are given off on a conical wave front, similarly to a sonic boom when an object exceeds the speed of sound.

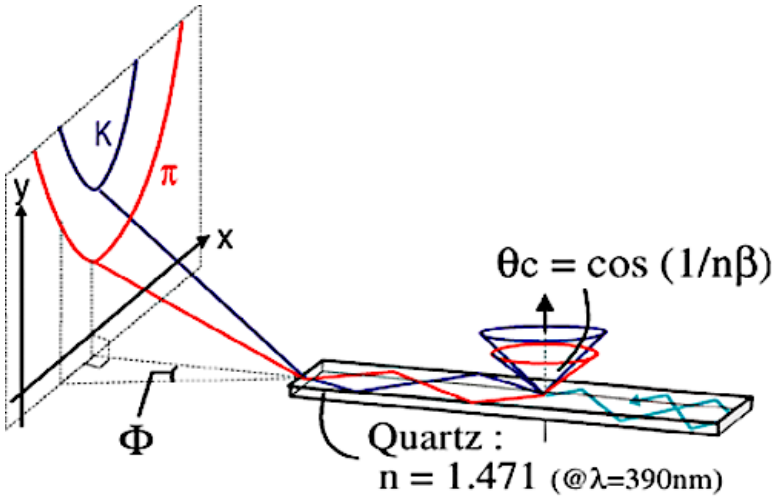

Figure 2: Cherenkov Radiation. A kaon and pion of the same momentum traversing the iTOP quartz will produce cones of Cherenkov radiation at different opening angles.

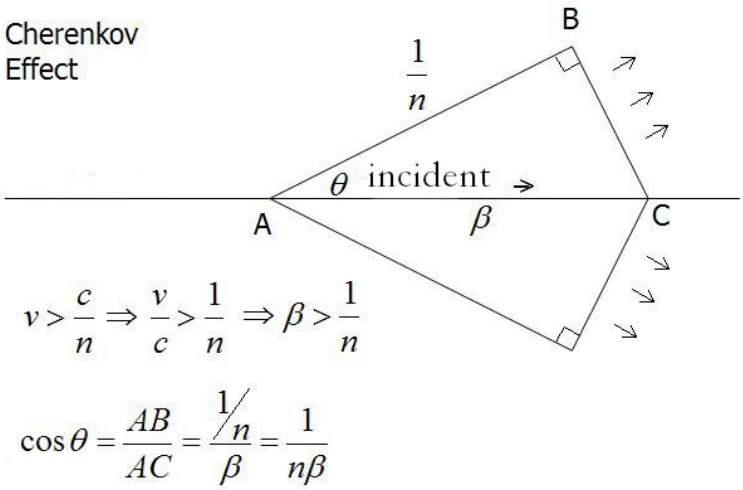

Figure 3: Opening Angle for Cherenkov Radiation. Diagram of the opening angle for Cherenkov radiation showing the angular dependence on the speed of the particle.

Now, it can be shown (see Figure 3.) that the angle that a photon makes with the incoming particle depends on its velocity as given by $\theta_c = cos(\frac{1}{n\beta})$, where $\beta = \frac{v}{c}$. Therefore, given the initial momentum of the particle, the angle can also determine the mass of the particle. It is then possible, given tracking information on the trajectory and momentum of the incident particle, to distinguish between different types of particles by determining the angle at which the Cherenkov photons deviate from the direction of the incident particle.

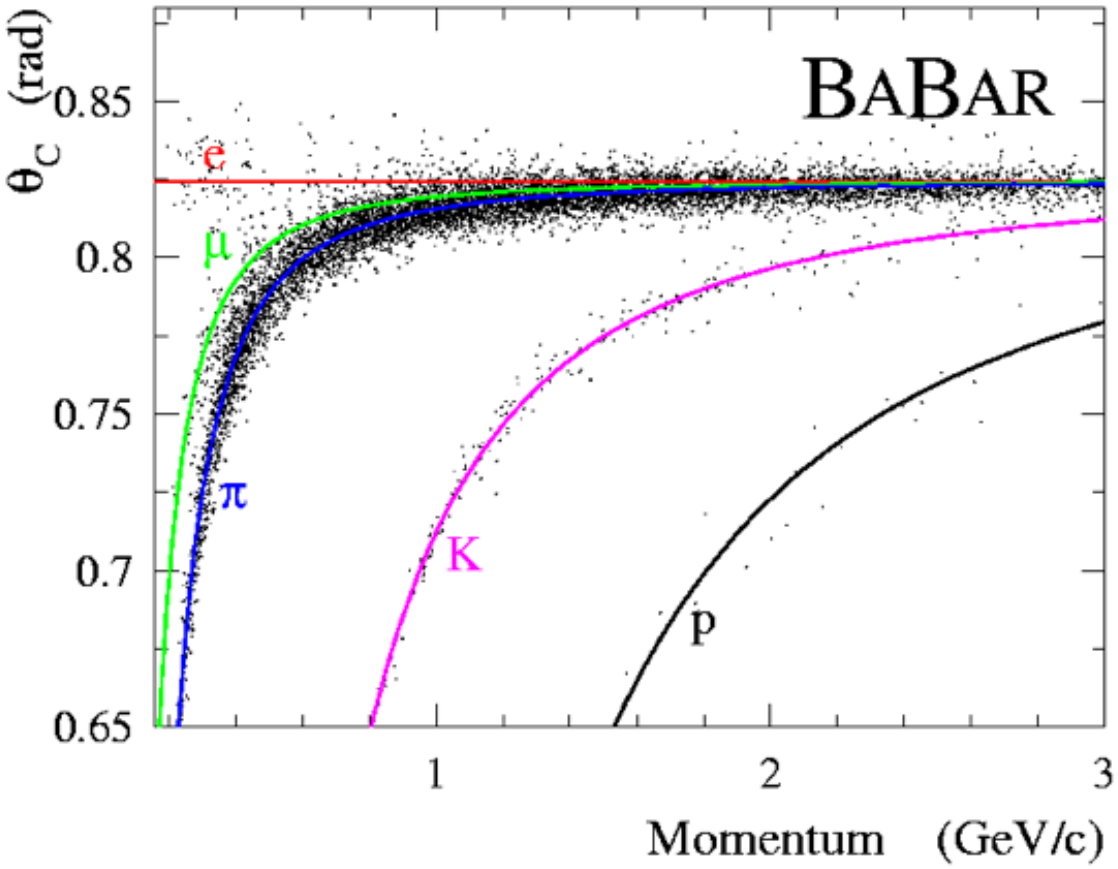

Figure 4: Opening Angle vs. Momentum. Opening Angle of the Cherenkov Photon in the fused quartz vs. Momentum at the BaBar experiment [3]. This distribution is almost identical to that obtained using data from the Belle II experiment. This plot demonstrates the difference in the opening angles of the photons produced in Cherenkov radiation for particles of different mass.

CHAPTER 3

THE BELLE II DETECTOR

The Belle II detector is an experiment that takes data at the Japanese high-energy accelerator complex KEK in Tsukuba, Japan [4, 5]. The accelerator collides 7 GeV electrons with 4 GeV positrons to produce large numbers of B mesons [6]. B mesons are very short-lived particles that contain a bottom quark or antiquark along with another quark. This experiment is trying to find and explain new physics beyond the standard model such as CP violation which can be used to explain the matter-antimatter asymmetry in the universe. There are many different sub-detectors in the Belle II experiment, but this project focuses mainly on the imaging time of propagation (iTOP) detector [7, 8, 9]. The iTOP is used for particle identification, especially to distinguish between pions and kaons. It is important to correctly identify these particles so that the B meson signal is as pure as possible since the B mesons decay preferentially to kaons. The iTOP is a long piece of quartz with a mirror on one end and a set of photodetectors on the other end.

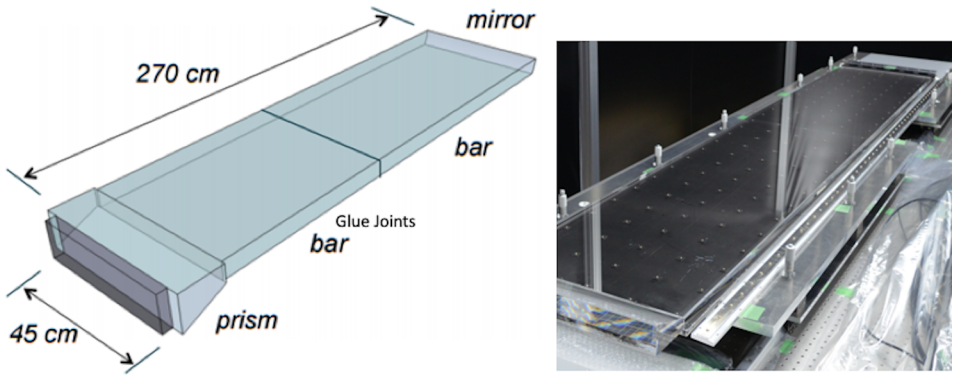

Figure 5: The iTOP Detector. Left: Rough dimensions of the fused quartz glass bar, prism and mirror of the iTOP. Right: A complete iTOP quartz assembly in fabrication.

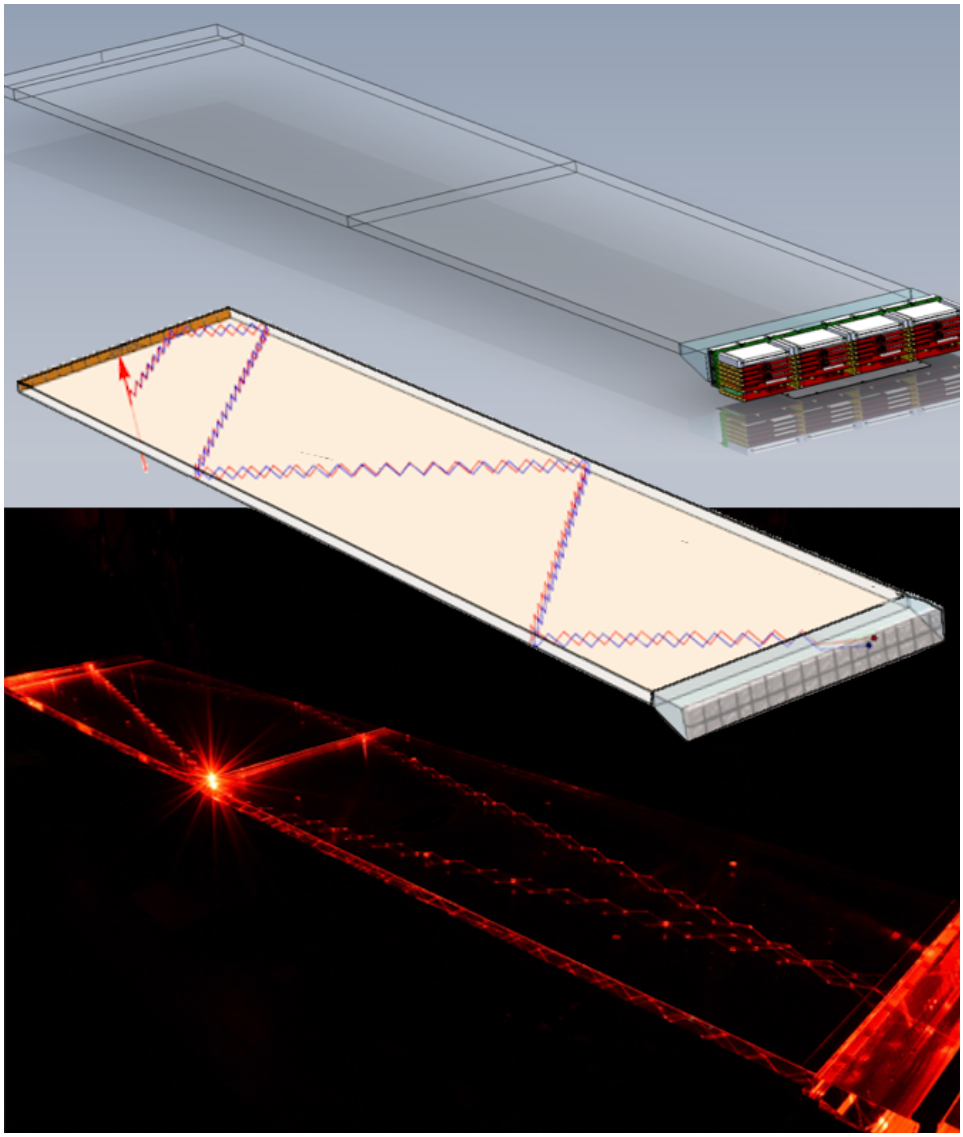

Figure 6: Photons in the iTOP Detector. (Bottom) Laser light is introduced into the iTOP quartz bar to observe the optical quality of the quartz bar and glue joints. The light undergoes many internal reflections. (Center) For comparison the internal reflections of Cherenkov photons from kaon and pion incident particles are shown schematically, (Top) also a schematic of the quartz, mirror and electronics.

When pions and kaons enter the iTOP, they produce cones of Cherenkov photons which propagate through the quartz and are detected at the end. From this detection, combined with the knowledge of the trajectory of the track, the time of flight information for all photons can be transformed into information about the opening angle. Since the angle between the photons and the particles depends on the mass of the particles, this can be used

to distinguish whether the particles were pions or kaons.

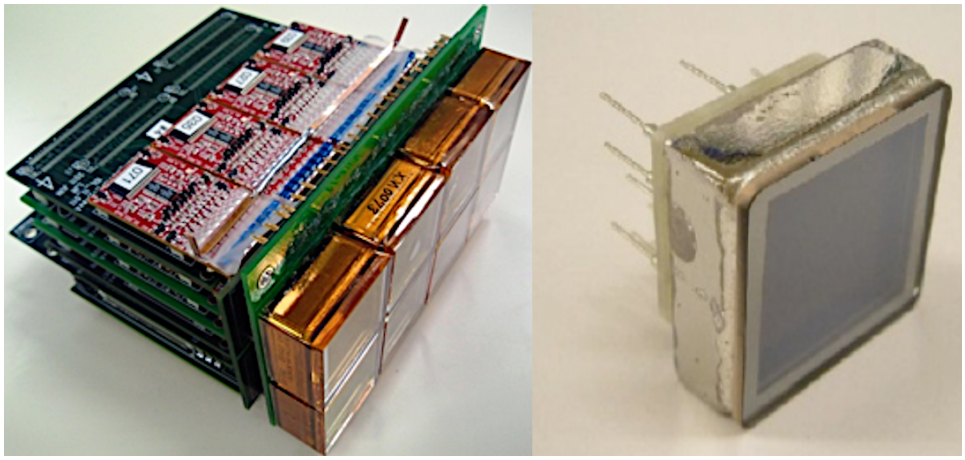

Figure 7: The Photomultiplier Tube. Pictures of the MC-PMTs attached to the end of the iTOP. Left is an array of 8 MC-PMTs attached to the electronics. Right is a single MC-PMT.

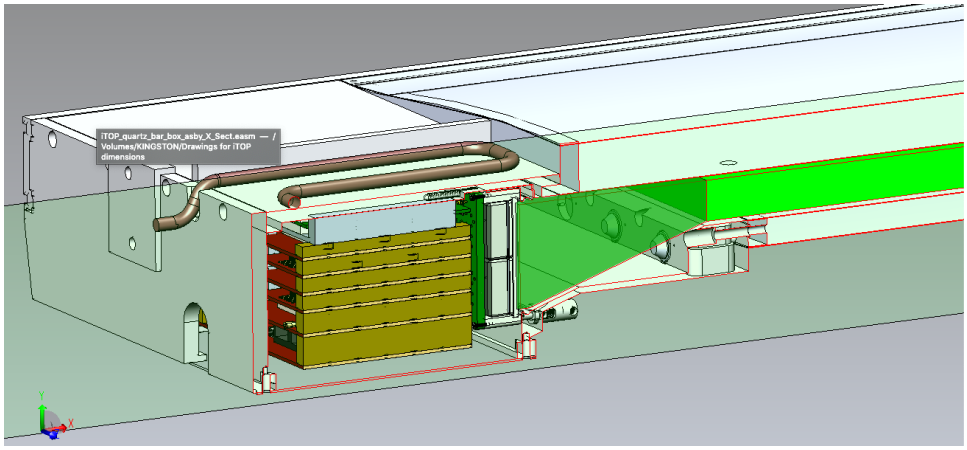

Figure 8: The iTOP Connected to the MC-PMTs. The figure shows how the iTOP bar is situated within the detector, connected to the MC-PMTs and the electronics.

CHAPTER 4

ANALYSIS OF ITOP OPTICS STUDIES

This thesis describes one of the four main steps in an overall program to determine the effect of the 1.5 T magnetic field [10] inside the Belle II detector on the efficiency for collecting Cherenkov photons in the iTOP detector. The Cherenkov photons produced by charged particles passing through the fused quartz of the iTOP travel by total internal reflection to photodetectors beyond the end of the quartz. At each bounce the photons are altered by reflection and change their polarization state to a different ellipticity. This is true even in the absence of a magnetic field. The Cherenkov photons are generated in a linearly polarized state. This is the basis for all simulations of the photons in Belle II software. However, in a magnetic field, the basis states are elliptically polarized waves of different phase velocity, and the reflection coefficients are different due to the field. In addition, the magnetic field strongly alters the polarization by rotating the polarization axis about the propagation direction, meaning that the existing Belle II simulation is based on inexact assumptions. This does not invalidate the key calculation of the time of flight vs. opening angle which has been expertly implemented for Belle II [11, 12]. However, inclusion of the generalized Faraday effect and proper reflection coefficients will reweight the individual photons because the probability that the photons will be transmitted beyond the end of the quartz bar is affected, and the probability of detection of the photons by the photocathode is also affected, since the photocathode has a quantum efficiency which depends strongly on the polarization state.

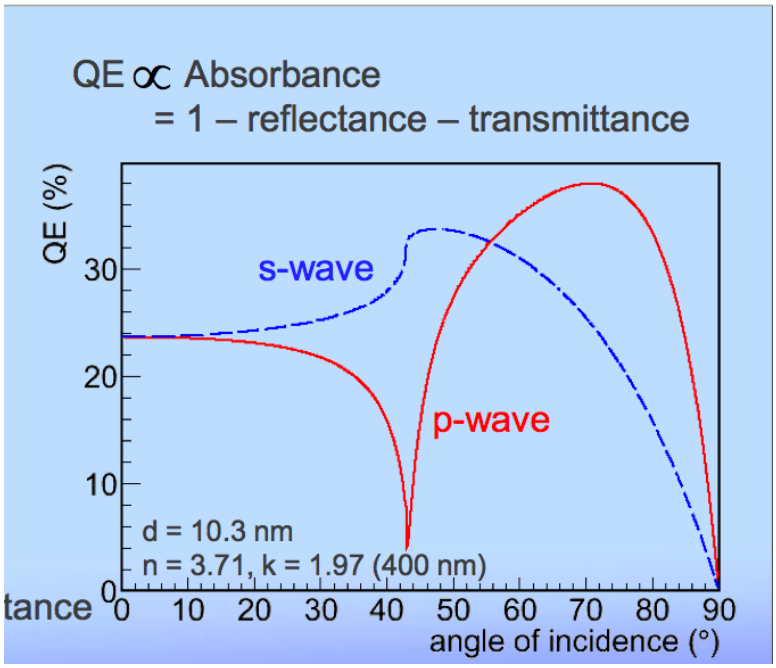

Figure 9: Quantum Efficiency vs. Incident Angle. The quantum efficiency of the iTOP MC-PMT photodiodes for s-wave (TE) and p-wave (TM) components of linear polarization as a function of angle of incidence. (Source: Kodai Matsuoka [13])

There are also prospects for subtle interference effects. At any reflection, even an internal reflection, part of the right-handed wave reflects as left-handed and vice versa. The two different helicity basis waves have minutely different indices of refraction, and therefore the outgoing right- and left-handed reflected waves come off at slightly different angles. The wave which eventually reaches the photocathode is a combination of right- and left-handed contributions with numerous different phases and as many possible directions. See Figure 10.

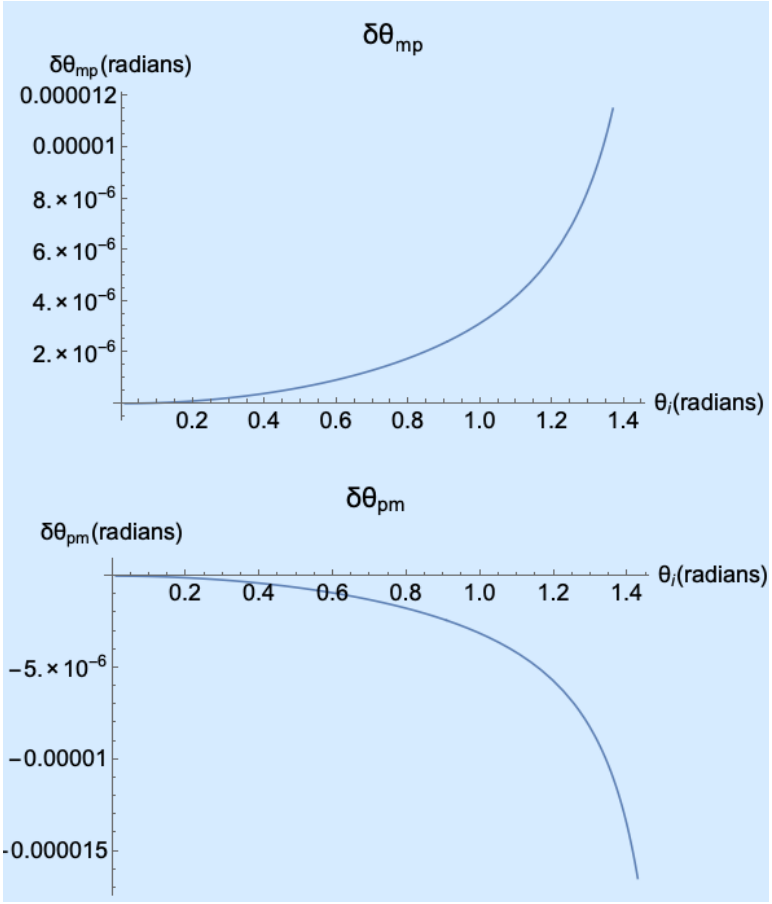

Figure 10: Angular Deviation from Incident Angle. The deviation δ_{pm} in radians due to a plus wave reflecting as minus handedness, and δ_{mp}, the deviation due to minus handedness reflecting as plus handed.

In the first stage of this project the general nature of the propagation of waves within the fused quartz was studied. The early literature developed in this context of the "generalized Faraday Effect" was developed both in the context of propagation of radio waves in the ionosphere and in optics. And the general formalism which gives the Appleton equation to determine the velocity of the waves of each handedness was used to find the relationship of the tabulated index of refraction in the fused quartz to permittivity components of the medium, and to predict the Verdet constants for the fused quartz (which has not been tabulated anywhere to our knowledge outside of our own Belle note 39 [1]).

In the second stage, samples of the fused quartz glass (Corning 7980) were purchased, and the Verdet constants for the glass was measured. The measured values were in good

agreement with the predictions of Belle note 39. This measurement is detailed in Samyukta Krishnamurthy's Honors Thesis [14]. At this stage the model of the generalized Faraday propagation was introduced into a Mathematica based Monte Carlo simulation to determine the effects of the magnetic field on the probability of a photon reaching the photocathode. A brief summary of these results is included below.

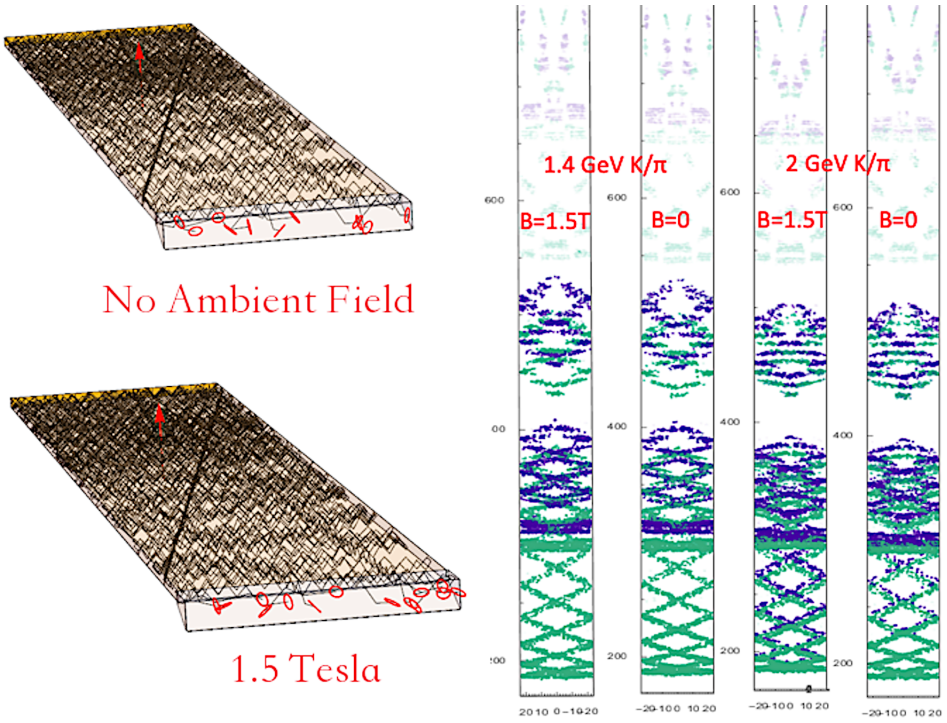

Figure 11: Effects of Faraday Rotation. The effects of the generalized Faraday rotation are seen in a standalone Monte Carlo build in Mathematica. The same photons have been generated with and without the Faraday rotation. Since the axis of polarization is rotated through many radians, the fraction of s-wave (TE) and p-wave (TM) is constantly changing, as well as changes in the ellipticity due to reflection. We see that different photons reach the MC-PMT with different ellipticity. Comparison of the naive Monte Carlo results at high momentum show that the chance of early arriving photons produced by incident kaons increases when the field is present.

In the next stage of the program, which this thesis details, reflection coefficients appropriate to strong magnetic fields were calculated. This was performed at an earlier stage under restricted conditions for which the glass-air interface was required to be parallel to the field. But these results are insufficient for simulating the iTOP, in which some of the latest and most crucial reflections come off of surfaces which are not parallel to the magnetic

field. There are beveled edges and truncated corners, but more importantly, the bottom of the prism is steeply sloped and the mirrored end of the quartz bar is a spherical surface. The prism surface was designed to permit an expansion of the bar to accommodate a double set of MC-PMTs at the readout end, but the additional position information comes at a cost of some difficulty in analyzing out-of-time hits due to trapping of photons in the prism.

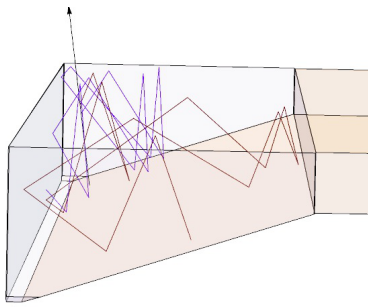

Figure 12: A Photon Trapped Within the Prism Volume.

This thesis details the special coordinate system and detailed calculations which led to correct reflection coefficients for all surfaces excepting at the mirrored surface at the end of the waveguide which is opposite the photodetector. That reflection requires separate treatment, outside of the current study due to the aluminum coating in the magnetic field. The solution of the reflection coefficients is described in detail below. Our group has previously calculated the reflection and transmission coefficients under the restricted assumption that the normal direction for the interface between the fused quartz and the outside nitrogen, at the point where reflection or transmission is about to occur, has no component along the ambient magnetic field. The main characteristic of this work is a new choice of coordinate system, motivated by the fact that the assumption of faces parallel to the magnetic field is invalid for many of the reflections, and consequently an entirely new style of solution is adopted.

In the remaining stage the treatment of the reflection coefficients in the mirrored surface are to be completed. Then the effects of ambient B field on inefficiencies, interference effects, etc., will be studied in our standalone Monte Carlo program. Finally the whole sweep

of the program is intended to be included as a set of special processes, particle classes, and physics lists in the GEANT4 [15] Monte Carlo, both for Belle II and for general use.

CHAPTER 5

MEASUREMENT OF THE VERDET CONSTANT

As part of Samyukta Krishnamurthy's Honors Thesis, the Verdet [14] constant was measured in the fused quartz Corning 7980, which is the material that makes up the main component of the iTOP detector. A sample of this material was purchased and placed inside a solenoid to produce a magnetic field. Next, a laser was shone through a polarizer in order to make the photons linearly polarized. Then, the light passed through the quartz with the magnetic field, was processed by an analyzer, and was measured by a photodiode.

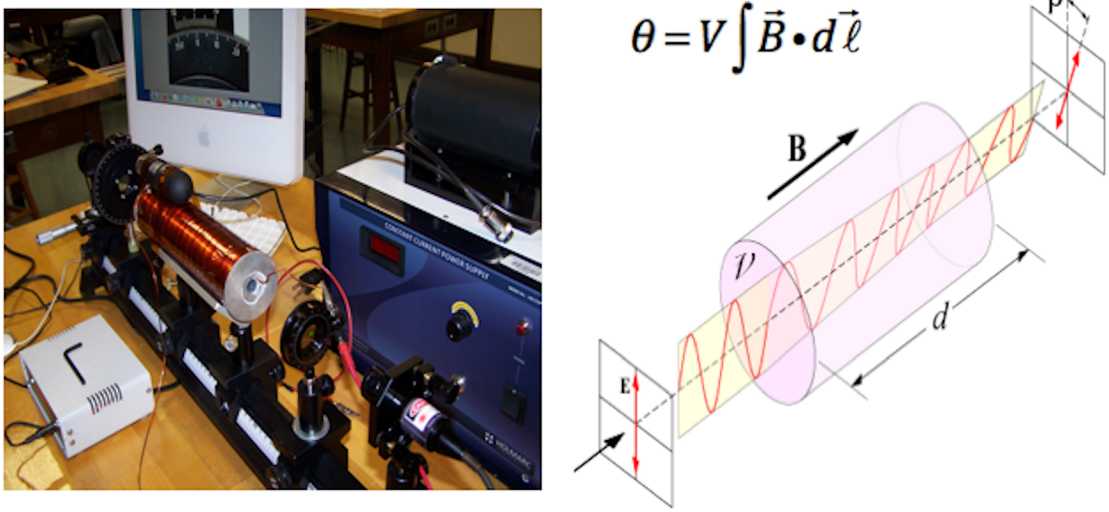

Figure 13: Faraday Effect Apparatus. The Faraday effect apparatus used for the determination of Verdet's constant in Corning 7980.

This allowed the rotation angle of the polarization to be measured which allowed for a measurement of the Verdet constant, which was found to be in good agreement with the theoretical predictions for various wavelengths.

The Faraday rotation data may be seen in Figure 14 a). It exhibits good linearity for each of the four wavelengths. In Figure 14 b) the measured Verdet constants for the four wavelengths are fit to a two-component parameterization of the form due to Tan and Arndt [16]. The precision is good over the range of our measured wavelengths.

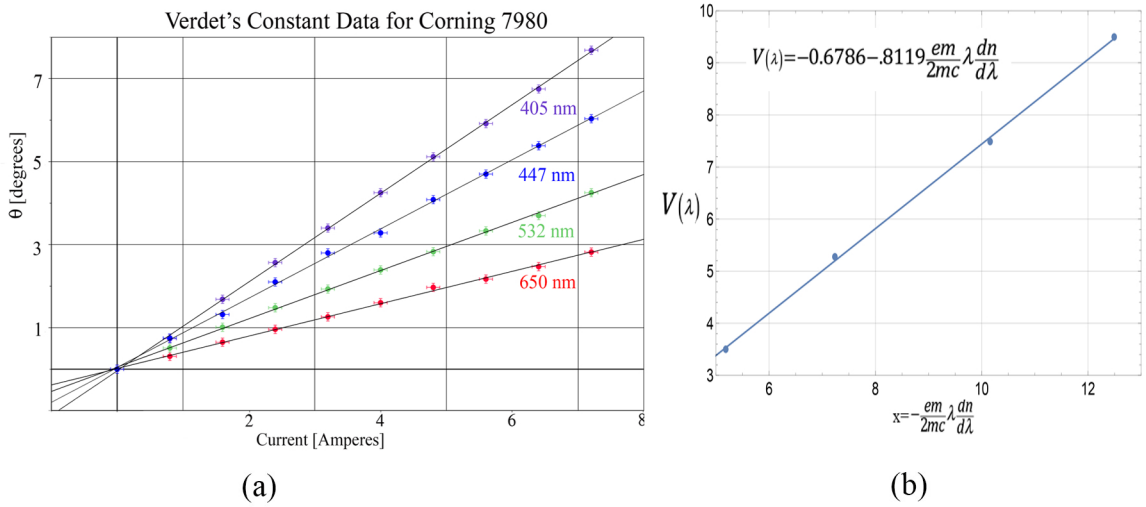

Figure 14: Verdet Constant Data. (a) Faraday rotation angle vs. magnetic field strength. (b) Verdet's constants data [14] for wavelengths 405 nm, 447 nm, 532 nm and 650 nm plotted against the two parameter Verdet's constant fit of the form derived by Tan and Arndt [16].

We used tabulated data for the index of refraction of Corning 7980 as a function of wavelength to extract our own permittivity tensor as described in Belle note 39 [1]. When we then used the calculated permittivity to calculate the Verdet constant as a function of frequency, it compared very well to our measurement of the Verdet constant data when we employed a two-parameter fit as suggested by Tan and Arndt [16] to improve the match to permittivity constants. Precise knowledge of the permittivity tensor is needed in order to get good reflection coefficients.

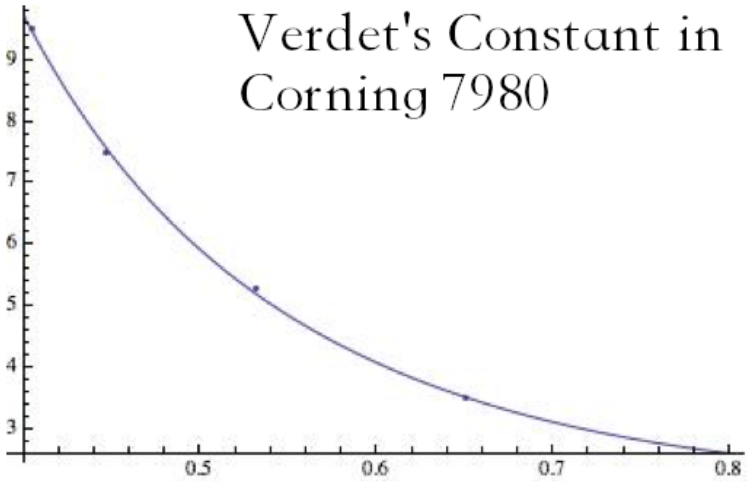

Figure 15: Verdet Constant Data Compared to Theory. A two parameter fit of the Verdet constant data to predictions based on our permittivity values. This is the basis for equation 2 above.

CHAPTER 6

DERIVATION OF THE PERMITTIVITY TENSOR, INDEX OF REFRACTION, AND ROTATION ANGLE

In many situations, the electric field vector and the electric displacement vector can be related by a scalar permittivity as $\vec{D} = \epsilon\vec{E}$. However, in some media, the permittivity is not isotropic and must be represented by a tensor. For gyro-electric media, i.e., isotropic media in the presence of an external magnetic field, the permittivity can be represented by

$$\begin{bmatrix} \epsilon_1 & i\epsilon_2 & 0 \\ -i\epsilon_2 & \epsilon_1 & 0 \\ 0 & 0 & \epsilon_3 \end{bmatrix}$$

Many advanced optics textbooks offer derivations of this form, and the associated Verdet constant in terms of frequency, the Larmor frequency of the medium (which for fused silica glass is about $B * 1.32 \times 10^{11}$), and resonant frequencies of the medium. The derivation found in Guenther is reproduced below [17].

The term "gyrotropic" is used for a medium that obeys the relationship between the displacement vector and the electric field:

$$D_j = \sum_{k=1}^{3} \epsilon_{jk} E_k + i(\vec{E} \times \vec{g})_j \tag{3}$$

where g is the gyration vector. The equation of motion is then

$$\frac{d^2\vec{r}}{dt^2} + \omega_0^2\vec{r} = -\frac{e}{m}(\vec{E} + \frac{d\vec{r}}{dt} \times \vec{B}) \tag{4}$$

Assuming that the ambient magnetic field and propagation vectors are along the z axis and casting the equation into circular motion, we get

$$\frac{d^2R_\pm}{dt^2} \mp \frac{e}{m} iB_z \frac{dR_\pm}{dt} + \omega_0^2 R_\pm = -\frac{e}{m} E_\pm \tag{5}$$

where R is the radial coordinate given by $R_\pm = x \pm iy$ and E is the electric field given by $E_\pm = E_x \pm iE_y$. Assuming a solution of the form

$$R_\pm = Ce^{i(\omega t - k_\pm z)}, \tag{6}$$

equation (4) becomes

$$-\omega^2 R_\pm \pm \frac{e}{m} B_z \omega R_\pm + \omega_0^2 R_\pm = -\frac{e}{m} E_\pm \tag{7}$$

which gives a solution of the form

$$R_\pm = \frac{\frac{e}{m} E_x}{(\omega_0^2 - \omega^2) \pm \frac{e}{m} B_z \omega} \tag{8}$$

which means the polarization vector is given by

$$P_\pm = \frac{N\frac{e^2}{m} E_\pm}{(\omega_0^2 - \omega^2) \pm \frac{e}{m} B_z \omega} \tag{9}$$

Now, let the Larmor precession frequency (the frequency at which the magnetic moment of the photon precesses) be

$$\omega_L = \frac{e}{2m} B_z \tag{10}$$

Then, we can write

$$(\omega_0 \pm \omega_L)^2 = \omega_0^2 \left[1 \pm 2\frac{\omega_L}{\omega_0} + (\frac{\omega_L}{\omega_0})^2 \right] \tag{11}$$

This shows that the magnetic field splits the resonant frequency into two new frequencies.

The index of refraction can then be found using

$$n_{\pm}^2 = 1 + \frac{\omega_p^2}{(\omega_0 \pm \omega_L)^2 - \omega^2} \tag{12}$$

This means that the two polarization states will travel through the medium at different velocities. Now, the index of refraction and the permittivity are related by

$$n = \sqrt{\frac{\epsilon}{\epsilon_0}} \tag{13}$$

The fact that there are more than one value for the index of refraction implies an anisotropic permittivity and a need for a permittivity tensor. This also means the polarization will be rotated through an angle

$$\theta = \frac{\pi L}{\lambda_0}(n_- - n_+) = \frac{\omega L}{c}(n_- - n_+) \tag{14}$$

which can be approximated by

$$\theta = \frac{\omega \omega_P^2 L}{c n_0} \frac{2\omega_0 \omega_L}{(\omega_0^2 + \omega_L^2 - \omega^2)^2 - 4\omega_0^2 \omega_L^2} \tag{15}$$

which is in agreement with equation (1).

CHAPTER 7

FINDING A PLANE WAVE SOLUTION FOR THE FIELDS

First we will seek a plane wave solution for the electric field in the form

$$\vec{E} = \vec{E}_0 e^{i(\omega t - \vec{k}\cdot\vec{x})} \tag{16}$$

Now, we know the fields have to satisfy Maxwell's equations which take the form

$$\begin{aligned}
\hat{k} \times \vec{E} &= \frac{\mu c}{n}\vec{H} \\
\hat{k} \times \vec{H} &= -\frac{c}{n}\overleftrightarrow{\epsilon}\cdot\vec{E} \\
\hat{k} \cdot \vec{H} &= 0 \\
\hat{k} \cdot (\overleftrightarrow{\epsilon}\cdot\vec{E}) &= 0
\end{aligned}$$

which lead to the set of equations relating the D and E fields

$$\begin{aligned}
\nabla \times (\nabla \times \vec{E}) &= -i\omega\mu_0 \nabla \times \vec{H} = \omega^2 \mu_0 D \\
\hat{k} \times (\vec{E} \times \hat{k}) &- \frac{1}{\epsilon_0 n^2} D = 0
\end{aligned}$$

The E and H fields can then be found using Maxwell's equations. These solutions for the E and H waves have been shown to satisfy the following equations.

$$\hat{k} \cdot \overleftrightarrow{\epsilon} \vec{E} = 0 \tag{17}$$

$$\hat{k} \cdot \vec{H} = 0 \tag{18}$$

$$\vec{E} - \frac{1}{\epsilon_0 n_{\pm}^2} \overleftrightarrow{\epsilon} \vec{E} = \hat{k} \times (\hat{k} \cdot \vec{E}) \tag{19}$$

$$\nabla \times \nabla \times \vec{E} = -\mu_0 \overleftrightarrow{\epsilon} \frac{\partial^2 \vec{E}}{\partial t^2} \tag{20}$$

$$\nabla \times \overleftrightarrow{\epsilon}^{-1} n_{\pm} (\nabla \times \vec{H}) = \nabla \times \frac{\partial \vec{E}}{\partial t} \tag{21}$$

$$-\hat{k} \times \left(\hat{k} \times \overleftrightarrow{\epsilon}^{-1} \cdot \vec{D} \right) - \frac{1}{\epsilon_0 n_{\pm}^2} \vec{D} = 0 \tag{22}$$

CHAPTER 8

CHANGING TO A NEW BASIS

One purpose of this study is to determine whether the inclusion of polarization related effects would improve the simulation of the iTOP by the GEANT4 Monte Carlo software package over the existing simulation. The current simulation of the Belle II iTOP uses a large fraction of the CPU time that Belle II GEANT4 simulation consumes due to the fact that it simulates optical photons in painstaking detail. (See Figure 16.) We sought a streamlined calculation for reflection and transmission coefficients that would work correctly for surfaces of the iTOP fused quartz that were oriented in arbitrary directions in comparison to the magnetic field. The coefficients were previously solved for the case of faces that were parallel to the field, but needed to be generalized, and sped up as well.

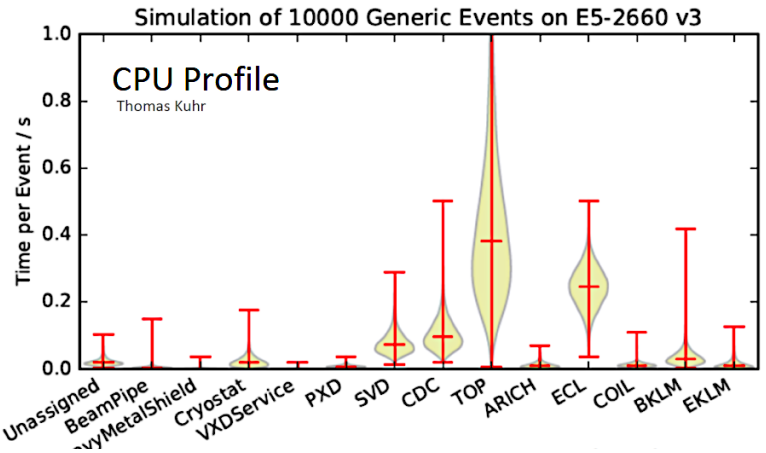

Figure 16: CPU Profile. CPU time for simulation of events by subsystem, for a sample of 10,000 events in GEANT4. Simulation of iTOP photons is the main contributor. Figure due to Thomas Kuhr [18], Belle II Collaboration.

It was necessary to cast the system into a new basis for efficiency and completeness of the solution. Prior to this work, a solution was found under the generalized Faraday effect in the x, y, z basis, in the particular case that the magnetic field aligns with the z axis, i.e., the longitudinal axis of the quartz bar. Reflection and transmission coefficients were found, but only for faces that were parallel to the B field. Initially, we followed a paper by Hillion[19], which also worked out a solution in the x, y, z basis, but had typographical errors. Correcting these errors and changing to a consistent unit system showed that they agreed with our results. There was very little guidance in the literature about the boundary value problem and analytic calculation of the coefficients, as much of it was concerned with radio waves and propagation in the ionosphere and used many approximations that would not hold in our system. The expressions for the coefficients found initially were very large and difficult to use in a Monte Carlo simulation, so we sought to find a more compact solution that could also be used for arbitrarily oriented axes of the interfaces. A thesis by Reichl [20] was used at first to find a new basis, which chose the direction of propagation as one of the basis vectors. Reichl used two approximations, that $\epsilon_{xx} = \epsilon_{zz}$, which we will refer to as approximation 1, and the approximation that

$$\left(\frac{\epsilon_{xy}}{\epsilon_{xx}}\right)^2 = 0, \tag{23}$$

which we will refer to as approximation 2. While the first approximation is commonly made and seemed to hold well, the second leads to inaccuracies in the difference between right-handed and left-handed indices of the order 10^{-6}, which may invalidate the polarization simulation after around 100 reflections. Without this second approximation, the Reichl form is not simple and we sought a new basis.

In order to satisfy the boundary conditions, another basis must be chosen. A basis was chosen with $\hat{\eta}$ and two vectors within the plane of incidence, one normal to the boundary, $\hat{n}$, and one along the boundary, $\hat{\zeta}$.

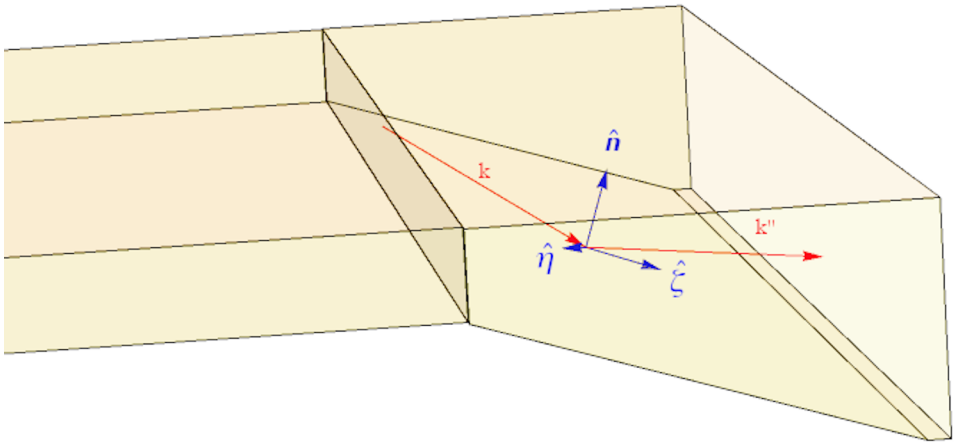

Figure 17: New Coordinate System. The coordinate system used to solve simultaneously for the reflection and transmission coefficients are shown. The $\hat{n}$ direction is an inward normal to the interface between fused quartz and nitrogen. The $\hat{\eta}$ direction is in the plane of the interface and perpendicular to plane formed by the incoming and outgoing waves. It corresponds to the TE direction for the electric field. The $\hat{\zeta}$ direction lies in the interface and is the projection of the propagation axis onto the plane of the interface.

We need to transform the permittivity from x, y, z coordinates to $\hat{n}$, $\hat{\eta}$, $\hat{\zeta}$ where

$$\hat{\eta} = \frac{\hat{k} \times \hat{n}}{|\hat{k} \times \hat{n}|} \tag{24}$$

$$\hat{\zeta} = \hat{n} \times \hat{\eta} \tag{25}$$

and the transformation is given by:

$$\overleftrightarrow{\epsilon}_{n\eta\zeta} = \begin{bmatrix} n_x & n_y & n_z \\ \eta_x & \eta_y & \eta_z \\ \zeta_x & \zeta_y & \zeta_z \end{bmatrix} \overleftrightarrow{\epsilon}_{xyz} = \epsilon_1 \begin{bmatrix} 1 & i\alpha\zeta_z & -i\alpha\eta_z \\ -i\alpha\zeta_z & 1 & i\alpha n_z \\ i\alpha\eta_z & -i\alpha n_z & 1 \end{bmatrix} \tag{26}$$

In the $\hat{n}$, $\hat{\eta}$, $\hat{\zeta}$ coordinate system, the curl becomes:

$$\nabla \times \overrightarrow{H} = \begin{bmatrix} \hat{n} & \hat{\eta} & \hat{\zeta} \\ (\hat{k} \cdot \hat{n}) & 0 & (\hat{\zeta} \cdot \hat{k}) \\ H_n & H_\eta & H_\zeta \end{bmatrix} \tag{27}$$

Some other definitions in the new basis include

$$\hat{k} = (-cos\theta_i, 0, sin\theta_i) \tag{28}$$

$$\hat{k}_{+TE} = k_{+TM} = (-cos\theta_t, 0, sin\theta_t) \tag{29}$$

where θ_i is the incident angle, θ_t is the transmitted angle, $sin\theta_t = \frac{n_+ sin\theta_i}{n_{box}}$, and $cos\theta_t = \sqrt{1 - \frac{n_+^2}{n_{box}^2} sin^2\theta_i}$.

$$\hat{k}_{-TE} = k_{-TM} = (-cos\theta_t, 0, sin\theta_t) \tag{30}$$

where $sin\theta_t = \frac{n_- sin\theta_i}{n_{box}}$, and $cos\theta_t = \sqrt{1 - \frac{n_-^2}{n_{box}^2} sin^2\theta_i}$ unless $\theta_i > \theta_c$. In that case, $cos\theta_t = i\sqrt{\frac{n_-^2}{n_{box}^2} sin^2\theta_i - 1}$. Now, if $\hat{n} \cdot \hat{z} = 0$, then $\theta_i = \theta_r$ and

$$\hat{k}_{pp} = \hat{k}_{mm} = (cos\theta_i, 0, sin\theta_i). \tag{31}$$

Otherwise, it is solved for by an iterative procedure by expanding around $\hat{k}_{pp} \approx \hat{k} - 2\hat{n}(\hat{k} \cdot \hat{n})$.

$$\hat{k}_{pm} = (cos\theta_{pm}, 0, sin\theta_{pm}) \tag{32}$$

$$\hat{k}_{mp} = (cos\theta_{mp}, 0, sin\theta_{mp}) \tag{33}$$

where $n_+ sin\theta_i = n_- sin\theta_{pm}$ and $n_- sin\theta_i = n_+ sin\theta_{mp}$.

$$|\hat{k} \times \hat{n}| = sin(\theta_i) \tag{34}$$

In this basis, the wave vector is

$$\hat{k}_{n\eta\zeta} = \left\{ (\hat{k} \cdot \hat{n}), 0, (\hat{\zeta} \cdot \hat{k}) \right\} \tag{35}$$

which can be shown to satisfy the equation

$$\hat{k}_{n\eta\zeta} \cdot \vec{D}_{n\eta\zeta} = 0 \tag{36}$$

As a consequence of equation 36, the electric displacement takes the form

$$\vec{D}_{n\eta\zeta} = \left\{ D_n, D_\eta, -D_n \frac{(\hat{k} \cdot \hat{n})}{(\hat{\zeta} \cdot \hat{k})} \right\} \tag{37}$$

which must satisfy the equation

$$\left[\left(-\hat{k} \times \hat{k} \times \right) \cdot \overleftrightarrow{\epsilon}^{-1} - \frac{1}{\epsilon_0 n_\pm^2} \right] \cdot \vec{D}_{n\eta\zeta} = 0 \tag{38}$$

Or, in vector form,

$$\left[\left(-\hat{k} \times \hat{k} \times \right) \cdot \left(\left(-1 + \alpha^2 \right) \epsilon_1 \right) \times \overleftrightarrow{\epsilon}^{-1} - \frac{\left(-1 + \alpha^2 \right) \epsilon 1}{\epsilon_0 n_\pm^2} \right] \cdot \begin{pmatrix} G_n(\hat{\zeta} \cdot \hat{k}) \\ G_\eta(\hat{\zeta} \cdot \hat{k}) \\ -G_n(\hat{k} \cdot \hat{n}) \end{pmatrix} = \begin{pmatrix} 0 \\ 0 \\ 0 \end{pmatrix} \tag{39}$$

where G_n is related to D_n by a constant. Now, in the new coordinate system,the expression that gives the $k \times k \times$ operator is

$$-\left(\hat{k}_{n\eta\zeta}\times\hat{k}_{n\eta\zeta}\times\right)=\begin{pmatrix}(\hat{\zeta}\cdot\hat{k})^2 & 0 & -(\hat{k}\cdot\hat{n})(\hat{\zeta}\cdot\hat{k})\\ 0 & 1 & 0\\ -(\hat{k}\cdot\hat{n})(\hat{\zeta}\cdot\hat{k}) & 0 & (\hat{k}\cdot\hat{n})^2\end{pmatrix}$$

and the inverse permittivity in this coordinate system becomes

$$\overleftrightarrow{\epsilon}_{n\eta\zeta}{}^{-1}=\begin{pmatrix}1-{n_z}^2\alpha^2 & \alpha\left(i\zeta_z+n_z\alpha\eta_z\right) & \alpha\left(n_z\alpha\zeta_z-i\eta_z\right)\\ \alpha\left(-i\zeta_z+n_z\alpha\eta_z\right) & 1-\alpha^2{\eta_z}^2 & \alpha\left(in_z+\alpha\zeta_z\eta_z\right)\\ \alpha\left(n_z\alpha\zeta_z+i\eta_z\right) & \alpha\left(-in_z+\alpha\zeta_z\eta_z\right) & 1-\alpha^2{\zeta_z}^2\end{pmatrix}$$

The solution of equation 39 gives the same results for the positive and negative plane wave solution as the Appleton equation:

$$n_+^2=\frac{\left(2-\left(1-{k_z}^2\right)\alpha^2+\alpha\sqrt{4{k_z}^2+\left(1-{k_z}^2\right)^2\alpha^2}\right)\epsilon_1}{2\epsilon_0} \tag{40}$$

$${n^2}_-=\frac{\left(2-\left(1-{k_z}^2\right)\alpha^2-\alpha\sqrt{4{k_z}^2+\left(1-{k_z}^2\right)^2\alpha^2}\right)\epsilon_1}{2\epsilon_0} \tag{41}$$

The positive plane wave solution is

$$\begin{pmatrix}-\frac{D_\zeta(\hat{\zeta}\cdot\hat{k})}{(\hat{k}\cdot\hat{n})}\\ \frac{D_\zeta\alpha(e_{1z}^2-\eta_z^2)-D_\zeta\sqrt{4k_z^2-(1+k_z^2)^2\alpha^2}}{2(\hat{k}\cdot\hat{n})(ik_z+e_{1z}\alpha\eta_z)}\\ D_\zeta\end{pmatrix}e^{-i\left(\frac{\omega\sqrt{n_{+0}^2}}{c}(\hat{n}(\hat{k}\cdot\hat{n})+\hat{\zeta}(\hat{\zeta}\cdot\hat{k}))\cdot\vec{r}-\omega t\right)} \tag{42}$$

and the negative solution is

$$\begin{pmatrix} -\frac{D_\zeta(\hat{\zeta}\cdot\hat{k})}{(\hat{k}\cdot\hat{n})} \\ \frac{D_\zeta\alpha(e1_z^2-\eta_z^2)-D_\zeta\sqrt{4k_z^2-(1+k_z^2)^2\alpha^2}}{2(\hat{k}\cdot\hat{n})(ik_z+e1_z\alpha\eta_z)} \\ D_\zeta \end{pmatrix} e^{-i\left(\frac{\omega\sqrt{n_{-0}^2}}{c}(\hat{n}(\hat{k}\cdot\hat{n})+\hat{\zeta}(\hat{\zeta}\cdot\hat{k}))\cdot\vec{r}-\omega t\right)} \tag{43}$$

The positive and negative solutions for the electric field are then given by

$$\begin{aligned}\vec{E} =& D_n \begin{pmatrix} -(\hat{\zeta}\cdot\hat{k})+\alpha(e1_z n_z\alpha+i(\hat{k}\cdot\hat{n})\eta_z)+P_\eta\alpha(-ik_z+e1_z\alpha\eta_z)(i\zeta_z+n_z\alpha\eta_z) \\ (\alpha(-ik_z+e1_z\alpha\eta_z)+P_\eta(-ik_z+e1_z\alpha\eta_z)(-1+\alpha^2\eta_z^2) \\ (\hat{k}\cdot\hat{n})+\alpha(e1_z\alpha\zeta_z+i(\hat{\zeta}\cdot\hat{k})\eta_z)+P_\eta\alpha(-ik_z+e1_z\alpha\eta_z)(-in_z+\alpha\zeta_z\eta_z) \end{pmatrix} \\ & e^{-i\left(\frac{\omega\sqrt{n_{-0}^2}}{c}(\hat{n}(\hat{k}\cdot\hat{n})+\hat{\zeta}(\hat{\zeta}\cdot\hat{k}))\cdot\vec{r}-\omega t\right)}\end{aligned} \tag{44}$$

and

$$\begin{aligned}\vec{E} =& D_n \begin{pmatrix} -(\hat{\zeta}\cdot\hat{k})+\alpha(e1_z n_z\alpha+i(\hat{k}\cdot\hat{n})\eta_z)+M_\eta\alpha(-ik_z+e1_z\alpha\eta_z)(i\zeta_z+n_z\alpha\eta_z) \\ (\alpha(-ik_z+e1_z\alpha\eta_z)+M_\eta(-ik_z+e1_z\alpha\eta_z)(-1+\alpha^2\eta_z^2) \\ (\hat{k}\cdot\hat{n})+\alpha(e1_z\alpha\zeta_z+i(\hat{\zeta}\cdot\hat{k})\eta_z)+M_\eta\alpha(-ik_z+e1_z\alpha\eta_z)(-in_z+\alpha\zeta_z\eta_z) \end{pmatrix} \\ & e^{-i\left(\frac{\omega\sqrt{n_{-0}^2}}{c}(\hat{n}(\hat{k}\cdot\hat{n})+\hat{\zeta}(\hat{\zeta}\cdot\hat{k}))\cdot\vec{r}-\omega t\right)}\end{aligned} \tag{45}$$

where $P_\eta = \frac{\sqrt{4k_z^2+(-1+k_z^2)^2\alpha^2}+\alpha(-1+k_z^2+2\eta_z^2)}{2(k_z^2+e1_z^2\alpha^2\eta_z^2)}$, $M_\eta = \frac{-\sqrt{4k_z^2+(-1+k_z^2)^2\alpha^2}+\alpha(-1+k_z^2+2\eta_z^2)}{2(k_z^2+e1_z^2\alpha^2\eta_z^2)}$, and $\alpha = \frac{\epsilon_2}{\epsilon_1}$. Note that the normalization of the fields here is arbitrary.

CHAPTER 9

BOUNDARY CONDITIONS AT THE INTERFACE

When a photon hits a face of the iTOP, part of the light is reflected and part of it is transmitted to the other side. For each right-handed incoming wave, with electric field denoted by E_{+0}, the reflected wave can either be right-handed or left-handed, denoted by E_{++} and E_{+-} respectively. The transmitted wave can be in either the transverse electric or transverse magnetic state, denoted by E_{+TE} and E_{+TM} respectively. There are similar denotations for the magnetic field, H. Now, the components of these fields must be the same across the boundary. Since the basis also needs to be consistent across the boundary, it will be pertinent to use the $n\eta\zeta$ basis. The equations that will be most useful are for the components parallel to the interface. This gives

$$\vec{E}_{+0} \cdot \hat{\eta} + r_{++}\vec{E}_{++} \cdot \hat{\eta} + r_{+-}\vec{E}_{+-} \cdot \hat{\eta} - t_{+TM}\vec{E}_{+TM} \cdot \hat{\eta} - t_{+TE}\vec{E}_{+TE} \cdot \hat{\eta} = 0 \tag{46}$$

$$\vec{E}_{+0} \cdot \hat{\zeta} + r_{++}\vec{E}_{++} \cdot \hat{\zeta} + r_{+-}\vec{E}_{+-} \cdot \hat{\zeta} - t_{+TM}\vec{E}_{+TM} \cdot \hat{\zeta} - t_{+TE}\vec{E}_{+TE} \cdot \hat{\zeta} = 0 \tag{47}$$

$$\vec{D}_{+0} \cdot \hat{n} + r_{++}\vec{D}_{++} \cdot \hat{n} + r_{+-}\vec{D}_{+-} \cdot \hat{n} - t_{+TM}\vec{D}_{+TM} \cdot \hat{n} - t_{+TE}\vec{D}_{+TE} \cdot \hat{n} = 0 \tag{48}$$

$$\vec{H}_{+0} \cdot \hat{\eta} + r_{++}\vec{H}_{++} \cdot \hat{\eta} + r_{+-}\vec{H}_{+-} \cdot \hat{\eta} - t_{+TM}\vec{H}_{+TM} \cdot \hat{\eta} - t_{+TE}\vec{H}_{+TE} \cdot \hat{\eta} = 0 \tag{49}$$

$$\vec{H}_{+0} \cdot \hat{\zeta} + r_{++}\vec{H}_{++} \cdot \hat{\zeta} + r_{+-}\vec{H}_{+-} \cdot \hat{\zeta} - t_{+TM}\vec{H}_{+TM} \cdot \hat{\zeta} - t_{+TE}\vec{H}_{+TE} \cdot \hat{\zeta} = 0 \tag{50}$$

Now, for the transverse electric wave, the electric field has no $\hat{\zeta}$ component and the magnetic field has no $\hat{\eta}$ component. Similarly for the transverse magnetic wave, the electric field has no $\hat{\eta}$ component and the magnetic field has no $\hat{\zeta}$ component.

These equations then become

$$\vec{E}_{+0} \cdot \hat{\eta} + r_{++}\vec{E}_{++} \cdot \hat{\eta} + r_{+-}\vec{E}_{+-} \cdot \hat{\eta} - t_{+TE}\vec{E}_{+TE} \cdot \hat{\eta} = 0 \tag{51}$$

$$\vec{E}_{+0} \cdot \hat{\zeta} + r_{++}\vec{E}_{++} \cdot \hat{\zeta} + r_{+-}\vec{E}_{+-} \cdot \hat{\zeta} - t_{+TM}\vec{E}_{+TM} \cdot \hat{\zeta} = 0 \tag{52}$$

$$\vec{H}_{+0} \cdot \hat{\eta} + r_{++}\vec{H}_{++} \cdot \hat{\eta} + r_{+-}\vec{H}_{+-} \cdot \hat{\eta} - t_{+TM}\vec{H}_{+TM} \cdot \hat{\eta} = 0 \tag{53}$$

$$\vec{H}_{+0} \cdot \hat{\zeta} + r_{++}\vec{H}_{++} \cdot \hat{\zeta} + r_{+-}\vec{H}_{+-} \cdot \hat{\zeta} - t_{+TE}\vec{H}_{+TE} \cdot \hat{\zeta} = 0 \tag{54}$$

Similarly, the boundary conditions can be written for an incoming wave with minus polarization.

$$\vec{E}_{-0} \cdot \hat{\eta} + r_{-+}\vec{E}_{-+} \cdot \hat{\eta} + r_{--}\vec{E}_{--} \cdot \hat{\eta} - t_{-TE}\vec{E}_{-TE} \cdot \hat{\eta} = 0 \tag{55}$$

$$\vec{E}_{-0} \cdot \hat{\zeta} + r_{-+}\vec{E}_{-+} \cdot \hat{\zeta} + r_{--}\vec{E}_{--} \cdot \hat{\zeta} - t_{-TM}\vec{E}_{-TM} \cdot \hat{\zeta} = 0 \tag{56}$$

$$\vec{H}_{-0} \cdot \hat{\eta} + r_{-+}\vec{H}_{-+} \cdot \hat{\eta} + r_{--}\vec{H}_{--} \cdot \hat{\eta} - t_{-TM}\vec{H}_{-TM} \cdot \hat{\eta} = 0 \tag{57}$$

$$\vec{H}_{-0} \cdot \hat{\zeta} + r_{-+}\vec{H}_{-+} \cdot \hat{\zeta} + r_{--}\vec{H}_{--} \cdot \hat{\zeta} - t_{-TE}\vec{H}_{-TE} \cdot \hat{\zeta} = 0 \tag{58}$$

Since the H field can be found from the E field using our form of Maxwell's equations, these equations can be used to solve for the reflection and transmission coefficients, r_{++}, r_{+-}, r_{-+}, r_{--}, t_{+TM}, t_{+TE}, t_{-TM}, and t_{-TE}.

Now, each component of the E and H fields can be broken up into real and imaginary parts to make the calculations simpler. The incoming electric field then becomes

$$\vec{E}_{+0} = (A + iB, C + iD, E + iF) \tag{59}$$

After expanding each component of the electric field and simplifying, the incoming field

becomes

$$\begin{aligned}\vec{E}_{+0} =& -(k_z + ie_{1z}\alpha\eta_z)(-2k_z((\hat{\zeta}\cdot\hat{k}) - i(\hat{k}\cdot\hat{n})\alpha\eta_z) + e_{1z}^2\alpha^2(-\zeta_z - in_z\alpha\eta_z)+ \\ & \alpha(\zeta_z - in_z\alpha\eta_z)(\sqrt{\alpha^2 + k_z^4\alpha^2 - 2k_z^2(-2+\alpha^2)} + \alpha\eta_z^2)+ \\ & 2e_{1z}\alpha(k_z n_z\alpha + \eta_z(i(\hat{\zeta}\cdot\hat{k}) + (\hat{k}\cdot\hat{n})\alpha\eta_z), \\ & i(k_z + ie_{1z}\alpha\eta_z)(2k_z^2\alpha + (\sqrt{\alpha^2 + k_z^4\alpha^2 - 2k_z^2(-2+\alpha^2)} + \alpha\eta_z^2) \\ & (-1 + \alpha^2\eta_z^2) + e_{1z}^2(\alpha + \alpha^3\eta_z^2)), \\ & -(k_z + ie_{1z}\alpha\eta_z)(2(\hat{k}\cdot\hat{n})(k_z - ie_{1z}\alpha\eta_z) + \alpha(e_{1z}^2\alpha(n_z - i\alpha\zeta_z\eta_z) + 2e_{1z}\alpha(k_z\zeta_z + (\hat{\zeta}\cdot\hat{k})\eta_z^2) \\ & -i(-2k_z(\hat{\zeta}\cdot\hat{k})\eta_z - in_z(\sqrt{\alpha^2 + k_z^4\alpha^2 - 2k_z^2(-2+\alpha^2)} + \alpha\eta_z^2) \\ & +\alpha\zeta_z\eta_z(\sqrt{\alpha^2 + k_z^4\alpha^2 - 2k_z^2(-2+\alpha^2)} + \alpha\eta_z^2))))\end{aligned} \tag{60}$$

Now, the H field can be found from the equation $\vec{k}\times\vec{E} = \omega\mu_0\vec{H}$ so that, using $\hat{k} = ((\hat{k}\cdot\hat{n}), 0, (\hat{\zeta}\cdot\hat{k}))$ for the n, η, ζ basis, $\vec{H}$ becomes

$$\vec{H}_{+0} = \frac{n}{c\mu_0}(-(\hat{\zeta}\cdot\hat{k})(C+iD), (\hat{\zeta}\cdot\hat{k})(A+iB) - (\hat{k}\cdot\hat{n})(E+iF), (\hat{k}\cdot\hat{n})(C+iD)) \tag{61}$$

In full form, the incoming H field is then

$$\begin{aligned}\vec{H}_{+0} =& \frac{n}{c\mu_0}((\hat{\zeta}\cdot\hat{k})(-ik_z + e_{1z}\alpha\eta_z)(2k_z^2\alpha+ \\ & (\sqrt{\alpha^2 + k_z^4\alpha^2 - 2k_z^2(-2+\alpha^2)} + \alpha\eta_z^2)(-1+\alpha^2\eta_z^2) + e_{1z}^2(\alpha + \alpha^3\eta_z^2)), \\ & (k_z + ie_{1z}\alpha\eta_z)(2(\hat{k}\cdot\hat{n})^2(k_z - ie_{1z}\alpha\eta_z) + (\hat{\zeta}\cdot\hat{k})(2k_z(\hat{\zeta}\cdot\hat{k}) + e_{1z}^2\alpha^2(\zeta_z + in_z\alpha\eta_z)- \\ & 2e_{1z}\alpha(k_z n_z\alpha + i(\hat{\zeta}\cdot\hat{k})\eta_z) + i\alpha(i\zeta_z + n_z\alpha\eta_z)(\sqrt{\alpha^2 + k_z^4\alpha^2 - 2k_z^2(-2+\alpha^2)} + \alpha\eta_z^2))+ \\ & (\hat{k}\cdot\hat{n})\alpha(2e_{1z}k_z\alpha\zeta_z + e1z^2\alpha(n_z - i\alpha\zeta_z\eta_z)(\sqrt{\alpha^2 + k_z^4\alpha^2 - 2k_z^2(-2+\alpha^2)} + \alpha\eta_z^2))), \\ & i(\hat{k}\cdot\hat{n})(k_z + ie_{1z}\alpha\eta_z)(2k_z^2\alpha + (\sqrt{\alpha^2 + k_z^4\alpha^2 - 2k_z^2(-2+\alpha^2)} + \alpha\eta_z^2)(-1+\alpha^2\eta_z^2)+ \\ & e_{1z}^2(\alpha + \alpha^3\eta_z^2)))\end{aligned} \tag{62}$$

Given the values for A, B, C, D, E, and F, it is possible to normalize the fields using

$$\vec{E}_{+0} = \frac{1}{N}(A_{+0} + iB_{+0}, C_{+0} + iD_{+0}, E_{+0} + iF_{+0}) \tag{63}$$

where $N = \sqrt{A^2 + B^2 + C^2 + D^2 + E^2 + F^2}$. The Normalizations of the D and H fields are determined by the normalization of E.

In order to crosscheck the validity of the fields, Maxwell's equations are used in the form

$$\vec{k} \cdot \vec{D} = 0 \tag{64}$$

$$\vec{k} \times \vec{H} = -\omega \vec{D} \tag{65}$$

$$\vec{k} \cdot \vec{H} = 0 \tag{66}$$

CHAPTER 10

RESULTS FOR THE COEFFICIENTS

In the presence of strong magnetic fields fused quartz is gyro-electric, and the basis states are not linearly polarized waves but counter-rotating elliptically polarized waves with different indices of refraction for each handedness. We derived reflection coefficients for right-handed to right-handed and left-handed to left-handed reflections, and also for right-handed to left-handed reflections and vice versa. Transmission coefficients for left- and right-handed waves to transmitted TM and transmitted TE waves are also found. There was not very much guidance in the literature for this step. On the one hand, we have to produce reflections of very high precision in order to get the phase changes correct for each handedness even after hundreds of bounces. Much of the literature is within the area of radio waves in the ionosphere and the approximations are far too large for our purposes. The case of optical literature is very often for limited cases of no use to this effort where more general solutions are needed.

Even consulting experts in gyrotropic media, we found that not much guidance could be offered beyond reaffirmation of the boundary conditions. Due to the dozens of internal reflections a photon will undergo, and the consequent fact that errors in the coefficients would be compounded by each new reflection, we set aside some standard approximations and performed an analytic solution to the boundary value problem in Mathematica to obtain the coefficients, up to approximation 1.

The results of this solution are given in full in the appendix. Some examples of the calculated coefficients are given by

$$
\begin{aligned}
r_{++} =&(NormP_{pp}(((\hat{k}\cdot\hat{n})_{pm}\sqrt{n_{-pm}^2}-(\hat{k}\cdot\hat{n})_{PT}n_{box})\xi_{m\eta pm}\\
&((\hat{k}\cdot\hat{n})_{PT}(\hat{\zeta}\cdot\hat{k})\sqrt{n_{+}^2}\xi_{pn}+(-(\hat{k}\cdot\hat{n})_{PT}(\hat{k}\cdot\hat{n})\sqrt{n_{+}^2}+n_{box})\xi_{p\zeta})-\\
&((\hat{k}\cdot\hat{n})\sqrt{n_{+}^2}-(\hat{k}\cdot\hat{n})_{PT}n_{box})((\hat{k}\cdot\hat{n})_{PT}(\hat{\zeta}\cdot\hat{k})_{pm}\sqrt{n_{-pm}^2}\xi_{mnpm}+\\
&(-(\hat{k}\cdot\hat{n})_{pm}(\hat{k}\cdot\hat{n})_{PT}\sqrt{n_{-pm}^2}+n_{box})\xi_{m\zeta pm})\xi_{p\eta}))/\\
&(NormP(-((\hat{k}\cdot\hat{n})_{pm}\sqrt{n_{-pm}^2}-(\hat{k}\cdot\hat{n})_{PT}n_{box})\xi_{m\eta pm}\\
&((\hat{k}\cdot\hat{n})_{PT}(\hat{\zeta}\cdot\hat{k})_{pp}\sqrt{n_{+pp}^2}\xi_{pnpp}+(-(\hat{k}\cdot\hat{n})_{pp}(\hat{k}\cdot\hat{n})_{PT}\sqrt{n_{+pp}^2}+n_{box})\xi_{p\zeta pp})+\\
&((\hat{k}\cdot\hat{n})_{pp}\sqrt{n_{+pp}^2}-(\hat{k}\cdot\hat{n})_{PT}n_{box})((\hat{k}\cdot\hat{n})_{PT}(\hat{\zeta}\cdot\hat{k})_{pm}\sqrt{n_{-pm}^2}\xi_{mnpm}+\\
&(-(\hat{k}\cdot\hat{n})_{pm}(\hat{k}\cdot\hat{n})_{PT}\sqrt{n_{-pm}^2}+n_{box})\xi_{m\zeta pm})\xi_{p\eta pp}))
\end{aligned}
\tag{67}
$$

$$
\begin{aligned}
r_{+-} =&(NormM_{pm}\left(\left((\hat{k}\cdot\hat{n})\sqrt{n_{+}^2}-(\hat{k}\cdot\hat{n})_{PT}n_{box}\right)\left((\hat{k}\cdot\hat{n})_{PT}(\hat{\zeta}\cdot\hat{k})_{pp}\sqrt{n_{+pp}^2}\xi_{pnpp}+\right.\right.\\
&\left.\left(-(\hat{k}\cdot\hat{n})_{pp}(\hat{k}\cdot\hat{n})_{PT}\sqrt{n_{+pp}^2}+n_{box}\right)\xi_{p\zeta pp}\right)\xi_{p\eta}-\left((\hat{k}\cdot\hat{n})_{pp}\sqrt{n_{+pp}^2}-(\hat{k}\cdot\hat{n})_{PT}n_{box}\right)\\
&\left.\left((\hat{k}\cdot\hat{n})_{PT}(\hat{\zeta}\cdot\hat{k})\xi_{pn}\sqrt{n_{+}^2}+\left(-(\hat{k}\cdot\hat{n})_{PT}(\hat{k}\cdot\hat{n})\sqrt{n_{+}^2}+n_{box}\right)\xi_{p\zeta}\right)\xi_{p\eta pp}\right)\Big)/\\
&\left(NormP\left(\left(-(\hat{k}\cdot\hat{n})_{pm}\sqrt{n_{-pm}^2}+(\hat{k}\cdot\hat{n})_{PT}n_{box}\right)\xi_{m\eta pm}((\hat{k}\cdot\hat{n})_{PT}(\hat{\zeta}\cdot\hat{k})_{pp}\right.\right.\\
&\left.\sqrt{n_{+pp}^2}\xi_{pnpp}+\left(-(\hat{k}\cdot\hat{n})_{pp}(\hat{k}\cdot\hat{n})_{PT}\sqrt{n_{+pp}^2}+n_{box}\right)\xi_{p\zeta pp}\right)+\\
&\left((\hat{k}\cdot\hat{n})_{pp}\sqrt{n_{+pp}^2}-(\hat{k}\cdot\hat{n})_{PT}n_{box}\right)\left((\hat{k}\cdot\hat{n})_{PT}(\hat{\zeta}\cdot\hat{k})_{pm}\sqrt{n_{-pm}^2}\xi_{mnpm}+\right.\\
&\left.\left.\left(-(\hat{k}\cdot\hat{n})_{pm}(\hat{k}\cdot\hat{n})_{PT}\sqrt{n_{-pm}^2}+n_{box}\right)\xi_{m\zeta pm}\right)\xi_{p\eta pp}\right)\Big)
\end{aligned}
\tag{68}
$$

where $(\hat{k}\cdot\hat{n})_{pm}=\hat{k}_{pm}\cdot\hat{n}$ and $NormP$, etc., are normalizations.

The results show that the plus to minus coefficients are essentially identical and that the new results for the coefficients agree with the previously tabulated results when restricted to the same conditions.

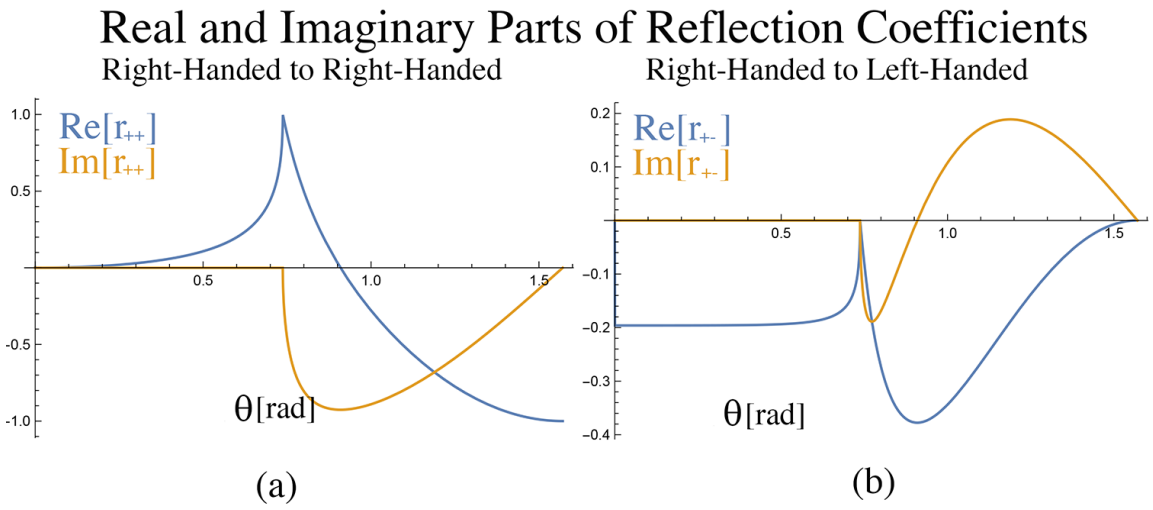

Figure 18: Plus Reflection Coefficients. Reflection coefficients for right-handed to right-handed (a) and right-handed to left-handed (b) elliptical waves in the iTOP for the plane of incidence parallel to the B field.

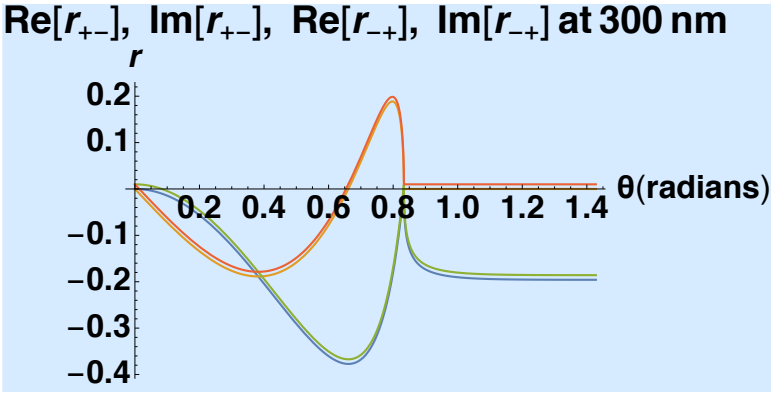

Figure 19: Reflection Coefficients Comparison. Reflection coefficients for right-handed to left-handed and left-handed to right-handed elliptical waves in the iTOP for the plane of incidence parallel to the $\vec{B}$ field. A small offset has been added to the latter to make both curves visible as they are indistinguishable in the unaltered plot.

CHAPTER 11

CONCLUSION

A new set of reflection and transmission coefficients was found using the boundary conditions for the electric and magnetic fields at the interface of the iTOP. They can be used for any face of the iTOP (except the mirror). These coefficients are shown to agree with previously calculated results when restricted to the same conditions. In addition, the electric and magnetic fields themselves are shown to satisfy the wave equations that govern the behavior of electromagnetic waves. The coefficients will be used in simulations to distinguish between kaons and pions which will help to reconstruct particle collisions in the Belle II experiment.

BIBLIOGRAPHY

[1] R. Kroeger, L. Cremaldi, D. Summers, and T. Jamerson, "The Effect of the Generalized Faraday Effect on Propagation of Polarization in the iTOP," Belle II Note 0039 (2016).

[2] P. A. Cherenkov, "Visible radiation produced by electrons moving in a medium with velocities exceeding that of light," Phys. Rev. **52** (1937) 378.

[3] I. Adam *et al.,* "The DIRC particle identification system for the BaBar experiment," Nucl. Instrum. Meth. **A538** (2005) 281.

[4] T. Abe *et al.,* "Belle II Technical Design Report," arXiv:1011.0352.

[5] E. Kou *et al.,* "The Belle II Physics Book," PTEP **2019** (2019) 123C01.

[6] Yukiyoshi Ohnishi *et al.,* "Accelerator design at SuperKEKB," PTEP **2013** (2013) 03A011.

[7] M. Akatsu *et al.,* "Time of propagation Cherenkov counter for particle identification," Nucl. Instrum. Meth. **A440** (2000) 124.

[8] K. Inami, "Development of a TOP counter for the super B factory," Nucl. Instrum. Meth. **A595** (2008) 96.

[9] Martin Bessner, "Performance of the Belle II imaging Time - of-Propagation (iTOP) detector in first collisions," https://doi.org/10.1016/j.nima.2019.06.059.

[10] M. Tan *et al.,* "Magnetic field mapping of the Belle solenoid," IEEE Trans. Nucl. Sci. **48** (2001) 900.

[11] K. Inami et. al. Nuclear Instruments and Methods in Physics Research A 440 (2000),1 24-135

[12] M. Staric Nuclear Instruments and Methods in Physics Research A 639, (2011) 252-255

[13] K. Matsuoka, "Design and Performance Study of the TOP Counter," 13th Vienna Conference on Instrumentation, 2013.

[14] S. Krishnamurthy, "Measurement of the Verdet Constant for a Previously Uncharacterized Fused Quartz Glass," Thesis, UMISS-HEP-2017-03.

[15] S. Agostinelli, J. Allison, K. A. Amako, J. Apostolakis, H. Araujo, P. Arce, M. Asai, D. Axen, S. Banerjee, G. Barrand GEANT4—a simulation toolkit Nucl. Instrum. Methods Phys. Res. Sect. A Accel. Spectrom. Detect. Assoc. Equip. 506 (2003) 250-303.

[16] C. Z. Tan and J. Arndt, Wavelength Dependance of the Faraday Effect in Glassy SiO2, Journal of Physics and Chemistry of Solids 60, 1681-1692 (1999).

[17] R. Guenther, *Modern Optics* (John Wiley & Sons, New York, 1990).

[18] Thomas Kuhr, "Belle II at the Start of Data Taking," EPJ Web Conf. **214** (2019) 09004

[19] P. Hillion, Harmonic Plane Wave Propagation In Gyroelectric Media, Jour. of Optics A, Pure and Applied Optics, 8 436-441 (2006).

[20] I. Reichl, Theoretical Investigations of Magneto-Optic Properties of Multilayer Systems, Ph.D. thesis, Technische Universität Wien, 2005.

APPENDIX

$$(\hat{k}\cdot\hat{n}) = k_x n_x + k_y n_y + k_z n_z \tag{69}$$

$$(\hat{\zeta}\cdot\hat{k}) = \zeta_x n_x + \zeta_y n_y + \zeta_z n_z \tag{70}$$

$$P_\eta = \frac{\left(\sqrt{4{k_z}^2 + \left(-1+{k_z}^2\right)^2\alpha^2} + \alpha\left(-1+{k_z}^2+2{\eta_z}^2\right)\right)}{2\left({k_z}^2 + {e_{1z}}^2\alpha^2{\eta_z}^2\right)} \tag{71}$$

$$M_\eta = \frac{\left(-\sqrt{4{k_z}^2 + \left(1-{k_z}^2\right)^2\alpha^2} + \alpha\left(-1+{k_z}^2+2{\eta_z}^2\right)\right)}{2\left({k_z}^2 + {e_{1z}}^2\alpha^2{\eta_z}^2\right)} \tag{72}$$

$$P\eta_{pp} = \frac{\left(\sqrt{4{k_{zpp}}^2 + \left(-1+{k_{zpp}}^2\right)^2\alpha^2} + \alpha\left(-1+{k_{zpp}}^2+2{\eta_z}^2\right)\right)}{2\left({k_{zpp}}^2 + {e1_{zpp}}^2\alpha^2{\eta_z}^2\right)} \tag{73}$$

$$P\eta_{mp} = \frac{\left(\sqrt{4{k_{zmp}}^2 + \left(-1+{k_{zmp}}^2\right)^2\alpha^2} + \alpha\left(-1+{k_{zmp}}^2+2{\eta_z}^2\right)\right)}{2\left({k_{zmp}}^2 + {e1_{zmp}}^2\alpha^2{\eta_z}^2\right)} \tag{74}$$

$$M\eta_{mm} = \frac{\left(-\sqrt{4{k_{zmm}}^2 + \left(-1+{k_{zmm}}^2\right)^2\alpha^2} + \alpha\left(-1+{k_{zmm}}^2+2{\eta_z}^2\right)\right)}{2\left({k_{zmm}}^2 + {e1_{zmm}}^2\alpha^2{\eta_z}^2\right)} \tag{75}$$

$$M\eta_{pm} = \frac{\left(-\sqrt{4{k_{zpm}}^2 + \left(-1+{k_{zpm}}^2\right)^2\alpha^2} + \alpha\left(-1+{k_{zpm}}^2+2{\eta_z}^2\right)\right)}{2\left({k_{zpm}}^2 + {e1_{zpm}}^2\alpha^2{\eta_z}^2\right)} \tag{76}$$

$$\tag{77}$$

$$(\hat{\zeta}\cdot\hat{k})_{pp} = \frac{\sqrt{n2Plus}}{\sqrt{n2Plus_{pp}}}(\hat{\zeta}\cdot\hat{k}) \tag{78}$$

$$(\hat{k}\cdot\hat{n})_{pp} = \sqrt{1-(\hat{\zeta}\cdot\hat{k})^2_{pp}} \tag{79}$$

$$(\hat{\zeta}\cdot\hat{k})_{mm} = \frac{\sqrt{n2Minus}}{\sqrt{n2Minus_{mm}}}(\hat{\zeta}\cdot\hat{k}) \tag{80}$$

$$(\hat{k}\cdot\hat{n})_{mm} = \sqrt{1-(\hat{\zeta}\cdot\hat{k})^2_{mm}} \tag{81}$$

$$\tag{82}$$

$$(\hat{\zeta}\cdot\hat{k})_{pm} = \frac{\sqrt{n2Plus}}{\sqrt{n2Plus_{pm}}}(\hat{\zeta}\cdot\hat{k}) \tag{83}$$

$$(\hat{k}\cdot\hat{n})_{pm} = \sqrt{1-(\hat{\zeta}\cdot\hat{k})^2_{pm}} \tag{84}$$

$$(\hat{\zeta}\cdot\hat{k})_{mp} = \frac{\sqrt{n2Minus}}{\sqrt{n2Minus_{mp}}}(\hat{\zeta}\cdot\hat{k}) \tag{85}$$

$$(\hat{k}\cdot\hat{n})_{mp} = \sqrt{1-(\hat{\zeta}\cdot\hat{k})^2_{mp}} \tag{86}$$

$$\tag{87}$$

$$e_{1z} = n_z(\hat{\zeta}\cdot\hat{k}) - (\hat{k}\cdot\hat{n})\zeta_z \tag{88}$$

$$e_{1zpp} = n_z(\hat{\zeta}\cdot\hat{k})_{pp} - (\hat{k}\cdot\hat{n})_{pp}\zeta_z \tag{89}$$

$$e_{1zmm} = n_z(\hat{\zeta}\cdot\hat{k})_{mm} - (\hat{k}\cdot\hat{n})_{mm}\zeta_z \tag{90}$$

$$e_{1zpm} = n_z(\hat{\zeta}\cdot\hat{k})_{pm} - (\hat{k}\cdot\hat{n})_{pm}\zeta_z \tag{91}$$

$$e_{1zmp} = n_z(\hat{\zeta}\cdot\hat{k})_{mp} - (\hat{k}\cdot\hat{n})_{mp}\zeta_z \tag{92}$$

$$\tag{93}$$

$$n2Plus \equiv n_+^2 = \frac{\left(2 - \left(1 - {k_z}^2\right)\alpha^2 + \alpha\sqrt{4{k_z}^2 + \left(1 - {k_z}^2\right)^2\alpha^2}\right)\epsilon_1}{2\epsilon_0} \tag{94}$$

$$n2Plus_{mp} \equiv {n^2}_{-+} = \frac{\left(2 - \left(1 - {k_{zmp}}^2\right)\alpha^2 + \alpha\sqrt{4{k_{zmp}}^2 + \left(1 - {k_{zmp}}^2\right)^2\alpha^2}\right)\epsilon_1}{2\epsilon_0} \tag{95}$$

$$n2Plus_{pp} \equiv {n^2}_{++} = \frac{\left(2 - \left(1 - {k_{zpp}}^2\right)\alpha^2 + \alpha\sqrt{4{k_{zpp}}^2 + \left(1 - {k_{zpp}}^2\right)^2\alpha^2}\right)\epsilon_1}{2\epsilon_0} \tag{96}$$

$$\tag{97}$$

$$\tag{98}$$

$$n2Minus \equiv {n^2}_{-} = \frac{\left(2 - \left(1 - {k_z}^2\right)\alpha^2 - \alpha\sqrt{4{k_z}^2 + \left(1 - {k_z}^2\right)^2\alpha^2}\right)\epsilon_1}{2\epsilon_0} \tag{99}$$

$$n2Minus_{mm} \equiv {n^2}_{--} = \frac{\left(2 - \left(1 - {k_{zmm}}^2\right)\alpha^2 - \alpha\sqrt{4{k_{zmm}}^2 + \left(1 - {k_{zmm}}^2\right)^2\alpha^2}\right)\epsilon_1}{2\epsilon_0} \tag{100}$$

$$n2Minus_{pm} \equiv {n^2}_{+-} = \frac{\left(2 - \left(1 - {k_{zpm}}^2\right)\alpha^2 - \alpha\sqrt{4{k_{zpm}}^2 + \left(1 - {k_{zpm}}^2\right)^2\alpha^2}\right)\epsilon_1}{2\epsilon_0} \tag{101}$$

$$\tag{102}$$

$$P\eta = \frac{\left(\sqrt{4{k_z}^2 + \left(-1 + {k_z}^2\right)^2\alpha^2} + \alpha\left(-1 + {k_z}^2 + 2{\eta_z}^2\right)\right)}{2\left({k_z}^2 + {e_{1z}}^2\alpha^2{\eta_z}^2\right)} \tag{103}$$

$$P\eta_{pp} = \frac{\left(\sqrt{4{k_{zpp}}^2 + \left(-1 + {k_{zpp}}^2\right)^2\alpha^2} + \alpha\left(-1 + {k_{zpp}}^2 + 2{\eta_z}^2\right)\right)}{2\left({k_{zpp}}^2 + {e_{1zpp}}^2\alpha^2{\eta_z}^2\right)} \tag{104}$$

$$P\eta_{mp} = \frac{\left(\sqrt{4{k_{zmp}}^2 + \left(-1 + {k_{zmp}}^2\right)^2\alpha^2} + \alpha\left(-1 + {k_{zmp}}^2 + 2{\eta_z}^2\right)\right)}{2\left({kz_{mp}}^2 + {e1_{zmp}}^2\alpha^2{\eta_z}^2\right)} \tag{105}$$

$$\tag{106}$$

$$M\eta = \frac{\left(-\sqrt{4{k_z}^2 + \left(-1 + {k_z}^2\right)^2\alpha^2} + \alpha\left(-1 + {k_z}^2 + 2{\eta_z}^2\right)\right)}{2\left({k_z}^2 + {e_{1z}}^2\alpha^2{\eta_z}^2\right)} \tag{107}$$

$$M\eta_{mm} = \frac{\left(-\sqrt{4{k_{zmm}}^2 + \left(-1 + {k_{zmm}}^2\right)^2\alpha^2} + \alpha\left(-1 + {k_{zmm}}^2 + 2{\eta_z}^2\right)\right)}{2\left({k_{zmm}}^2 + {e_{1zmm}}^2\alpha^2{\eta_z}^2\right)} \tag{108}$$

$$M\eta_{pm} = \frac{\left(-\sqrt{4{k_{zpm}}^2 + \left(-1 + {k_{zpm}}^2\right)^2\alpha^2} + \alpha\left(-1 + {k_{zpm}}^2 + 2{\eta_z}^2\right)\right)}{2\left({k_{zpm}}^2 + {e_{1zpm}}^2\alpha^2{\eta_z}^2\right)} \tag{109}$$

$$\tag{110}$$

$$AA = D_n \left(e_{1z} n_z \alpha^2 - (\hat{\zeta} \cdot \hat{k}) + P_\eta \alpha \left(k_z \zeta_z + e_{1z} n_z \alpha^2 {\eta_z}^2 \right) \right) \tag{111}$$

$$BB = D_n \left((\hat{k} \cdot \hat{n}) \alpha \eta_z - P_\eta \alpha^2 \left(k_z n_z - e_{1z} \zeta_z \right) \eta_z \right) \tag{112}$$

$$CC = D_n e_{1z} \alpha \eta_z \left(\alpha + P_\eta \left(-1 + \alpha^2 {\eta_z}^2 \right) \right) \tag{113}$$

$$DD = -D_n k_z \left(\alpha - P_\eta \left(1 - \alpha^2 {\eta_z}^2 \right) \right) \tag{114}$$

$$EE = D_n \left((\hat{k} \cdot \hat{n}) + \alpha \left(e_{1z} \alpha \zeta_z + P_\eta \left(-k_z n_z + e_{1z} \alpha^2 \zeta_z {\eta_z}^2 \right) \right) \right) \tag{115}$$

$$FF = D_n \alpha \left((\hat{\zeta} \cdot \hat{k}) - P_\eta \alpha \left(e_{1z} n_z + k_z \zeta_z \right) \right) \eta_z \tag{116}$$

$$\tag{117}$$

$$AApp = Dn \left(e_{1z} n_z \alpha^2 - (\hat{\zeta} \cdot \hat{k})_{pp} + P\eta_{pp} \alpha \left(k_{zpp} Mp_{pp} \zeta_z + e_{1zpp} n_z \alpha^2 {\eta_z}^2 \right) \right) \tag{118}$$

$$BBpp = Dn \left((\hat{k} \cdot \hat{n})_{pp} \alpha \eta_z - P\eta_{pp} \alpha^2 \left(k_{zpp} n_z - e_{1zpp} \zeta_z \right) \eta_z \right) \tag{119}$$

$$CCpp = Dn e_{1zpp} \alpha \eta_z \left(\alpha - P\eta_{pp} \left(1 - \alpha^2 {\eta_z}^2 \right) \right) \tag{120}$$

$$DDpp = -Dn k_{zpp} \left(\alpha - P\eta_{pp} \left(1 + \alpha^2 {\eta_z}^2 \right) \right) \tag{121}$$

$$EEpp = Dn \left((\hat{k} \cdot \hat{n})_{pp} + \alpha \left(e_{1zpp} \alpha \zeta_z + P\eta_{mp} \left(-k_{zpp} n_z + e_{1zpp} \alpha^2 \zeta_z {\eta_z}^2 \right) \right) \right) \tag{122}$$

$$FFpp = Dn\alpha \left((\hat{\zeta} \cdot \hat{k})_{pp} - P\eta_{pp} \alpha \left(e_{1zpp} n_z + k_{zpp} \zeta_z \right) \right) \eta_z \tag{123}$$

$$\tag{124}$$

$$AAmp = Dn\left(e_{1z}n_z\alpha^2 - (\hat{\zeta}\cdot\hat{k})_{mp} + P\eta_{mp}\alpha\left(k_{zmp}Mp_{mp}\zeta_z + e_{1zmp}n_z\alpha^2{\eta_z}^2\right)\right) \tag{125}$$

$$BBmp = Dn\left((\hat{k}\cdot\hat{n})_{mp}\alpha\eta_z - P\eta_{mp}\alpha^2\left(k_{zmp}n_z - e_{1zmp}\zeta_z\right)\eta_z\right) \tag{126}$$

$$CCmp = Dne_{1zmp}\alpha\eta_z\left(\alpha - P\eta_{mp}\left(1 - \alpha^2{\eta_z}^2\right)\right) \tag{127}$$

$$DDmp = -Dnk_{zmp}\left(\alpha - P\eta_{mp}\left(1 + \alpha^2{\eta_z}^2\right)\right) \tag{128}$$

$$EEmp = Dn\left((\hat{k}\cdot\hat{n})_{mp} + \alpha\left(e_{1zmp}\alpha\zeta_z + P\eta_{mp}\left(-k_{zmp}n_z + e_{1zmp}\alpha^2\zeta_z{\eta_z}^2\right)\right)\right) \tag{129}$$

$$FFmp = Dn\alpha\left((\hat{\zeta}\cdot\hat{k})_{mp} - P\eta_{mp}\alpha\left(e_{1zmp}n_z + k_{zmp}\zeta_z\right)\right)\eta_z \tag{130}$$

$$\tag{131}$$

$$AAM = Dn\left(e_{1z}n_z\alpha^2 - (\hat{\zeta}\cdot\hat{k}) + M\eta\alpha\left(k_z\zeta_z + e_{1z}n_z\alpha^2{\eta_z}^2\right)\right) \tag{132}$$

$$BBM = Dn\left((\hat{k}\cdot\hat{n})\alpha\eta_z - M\eta\alpha^2\left(k_zn_z - e_{1z}\zeta_z\right)\eta_z\right) \tag{133}$$

$$CCM = Dne_{1z}\alpha\eta_z\left(\alpha - M\left(-1 - \alpha^2{\eta_z}^2\right)\right) \tag{134}$$

$$DDM = -Dnk_z\left(\alpha - M\eta\left(1 - \alpha^2{\eta_z}^2\right)\right) \tag{135}$$

$$EEM = Dn\left((\hat{k}\cdot\hat{n}) + \alpha\left(e_{1z}\alpha\zeta_z + M\eta\left(-k_zn_z + e_{1z}\alpha^2\zeta_z{\eta_z}^2\right)\right)\right) \tag{136}$$

$$FFM = Dn\alpha\left((\hat{\zeta}\cdot\hat{k}) - M\eta\alpha\left(e_{1z}n_z + k_z\zeta_z\right)\right)\eta_z \tag{137}$$

$$\tag{138}$$

$$AAMmm = Dn\left(e_{1zmm}n_z\alpha^2 - (\hat{\zeta}\cdot\hat{k})_{mm} + M\eta_{mm}\alpha\left(k_{zmm}\zeta_z + e_{1zmm}n_z\alpha^2{\eta_z}^2\right)\right) \tag{139}$$

$$BBMmm = Dn\left((\hat{k}\cdot\hat{n})_{mm}\alpha\eta_z - M\eta_{mm}\alpha^2\left(k_{zmm}n_z - e_{1zmm}\zeta_z\right)\eta_z\right) \tag{140}$$

$$CCMmm = Dne1_{zmm}\alpha\eta_z\left(\alpha - M\eta_{mm}\left(1-\alpha^2{\eta_z}^2\right)\right) \tag{141}$$

$$DDMmm = -Dnk_{zmm}\left(\alpha + M\eta_{mm}\left(1-\alpha^2{\eta_z}^2\right)\right) \tag{142}$$

$$EEMmm = Dn\left((\hat{k}\cdot\hat{n})_{mm} + \alpha\left(e_{1zmm}\alpha\zeta_z + M\eta_{mm}\left(-k_{zmm}n_z + e_{1zmm}\alpha^2\zeta_z{\eta_z}^2\right)\right)\right) \tag{143}$$

$$FFMmm = Dn\alpha\left((\hat{\zeta}\cdot\hat{k})_{mm} - M\eta_{mm}\alpha\left(e_{1zmm}n_z + k_{zmm}\zeta_z\right)\right)\eta_z \tag{144}$$

$$\tag{145}$$

$$AAMpm = Dn\left(e_{1zpm}n_z\alpha^2 - (\hat{\zeta}\cdot\hat{k})_{pm} + M\eta_{pm}\alpha\left(k_{zpm}\zeta_z + e_{1zpm}n_z\alpha^2{\eta_z}^2\right)\right) \tag{146}$$

$$BBMpm = Dn\left((\hat{k}\cdot\hat{n})_{pm}\alpha\eta_z - M\eta_{pm}\alpha^2\left(k_{zpm}n_z - e_{1zpm}\zeta_z\right)\eta_z\right) \tag{147}$$

$$CCMpm = Dne_{1zpm}\alpha\eta_z\left(\alpha 1 M\eta_{pm}\left(1-\alpha^2{\eta_z}^2\right)\right) \tag{148}$$

$$DDMpm = -Dnk_{zpm}\left(\alpha - M\eta_{pm}\left(1-\alpha^2{\eta_z}^2\right)\right) \tag{149}$$

$$EEMpm = Dn\left((\hat{k}\cdot\hat{n})_{pm} + \alpha\left(e_{1zpm}\alpha\zeta_z + M\eta_{pm}\left(-k_{zpm}n_z + e_{1zpm}\alpha^2\zeta_{zz}{\eta_z}^2\right)\right)\right) \tag{150}$$

$$FFMpm = Dn\alpha\left((\hat{\zeta}\cdot\hat{k})_{pm} - M\eta_{pm}\alpha\left(e_{1zpm}n_z + k_{zpm}\zeta_z\right)\right)\eta_z \tag{151}$$

$$\tag{152}$$

$$\frac{(CC+iDD)}{NormP}+\frac{(CCpp+iDDpp)}{NormPpp}rpp+$$
$$\frac{(CCMpm+iDDMpm)}{NormMpm}rpm-\frac{EPTE}{NormPTE}tpte=0$$
$$\frac{(EE+iFF)}{NormP}+\frac{(EEpp+iFFpp)}{NormPpp}rpp+$$
$$\frac{(EEMpm+iFFMpm)}{NormMpm}rpm+\frac{EPTM(\hat{k}\cdot\hat{n})PT}{NormPTM}tptm=0$$
$$\frac{\sqrt{n2Plus}}{c\mu_0}\left((\hat{\zeta}\cdot\hat{k})\frac{(AA+iBB)}{NormP}-(\hat{k}\cdot\hat{n})\frac{(EE+iFF)}{NormP}\right)+$$
$$\frac{\sqrt{n2Pluspp}}{c\mu_0}\left((\hat{\zeta}\cdot\hat{k})pp\frac{(AApp+iBBpp)}{NormPpp}-(\hat{k}\cdot\hat{n})pp\frac{(EEpp+iFFpp)}{NormPpp}\right)rpp+$$
$$\frac{\sqrt{n2Minuspm}}{c\mu_0}\Bigg((\hat{\zeta}\cdot\hat{k})pm\frac{(AAMpm+iBBMpm)}{NormMpm}-$$
$$(\hat{k}\cdot\hat{n})pm\frac{(EEMpm+iFFMpm)}{NormMpm}\Bigg)rpm-\frac{EPTMn_{box}}{cNormPTM\mu_0}tptm=0$$
$$\frac{\sqrt{n2Plus}}{c\mu_0}(\hat{k}\cdot\hat{n})\frac{(CC+iDD)}{NormP}+\frac{\sqrt{n2Pluspp}}{c\mu_0}(\hat{k}\cdot\hat{n})pp\frac{(CCpp+iDDpp)}{NormPpp}rpp+$$
$$\frac{\sqrt{n2Minuspm}}{c\mu_0}(\hat{k}\cdot\hat{n})pm\frac{(CCMpm+iDDMpm)}{NormMpm}rpm-\frac{EPTE(\hat{k}\cdot\hat{n})PTn_{box}}{cNormPTE\mu_0}tpte=0 \tag{153}$$

$$\xi_{pn} = AA + iBB \tag{154}$$

$$\xi_{p\eta} = CC + iDD \tag{155}$$

$$\xi_{p\varsigma} = EE + iFF \tag{156}$$

$$\xi_{mn} = AAM + iBBM \tag{157}$$

$$\xi_{m\eta} = CCM + iDDM \tag{158}$$

$$\xi_{m\varsigma} = EEM + iFFM \tag{159}$$

$$\xi_{pnpp} = AA_{pp} + iBB_{pp} \tag{160}$$

$$\xi_{p\eta pp} = CC_{pp} + iDD_{pp} \tag{161}$$

$$\xi_{p\varsigma pp} = EE_{pp} + iFF_{pp} \tag{162}$$

$$\xi_{mnmm} = AAM_{mm} + iBBM_{mm} \tag{163}$$

$$\xi_{m\eta mm} = CCM_{mm} + iDDM_{mm} \tag{164}$$

$$\xi_{m\varsigma mm} = EEM_{mm} + iFFM_{mm} \tag{165}$$

$$\tag{166}$$

$$\xi_{pnmp} = AA_{mp} + iBB_{mp} \tag{167}$$

$$\xi_{p\eta mp} = CC_{mp} + iDD_{mp} \tag{168}$$

$$\xi_{p\varsigma mp} = EE_{mp} + iFF_{mp} \tag{169}$$

$$\xi_{mnpm} = AAM_{pm} + iBBM_{pm} \tag{170}$$

$$\xi_{m\eta pm} = CCM_{pm} + iDDM_{pm} \tag{171}$$

$$\xi_{m\varsigma pm} = EEM_{pm} + iFFM_{pm} \tag{172}$$

$$\tag{173}$$

$$
\begin{aligned}
&r_{++} = \\
&NormP_{pp}\left(\left((\hat{k}\cdot\hat{n})_{pm}\sqrt{n2Minus_{pm}}-(\hat{k}\cdot\hat{n})_{PT}n_{box}\right)\xi_{m\eta pm}\left((\hat{k}\cdot\hat{n})_{PT}\sqrt{n2Plus}(\hat{\zeta}\cdot\hat{k})\xi_{pn}+\right.\right.\\
&\left.\left(-(\hat{k}\cdot\hat{n})(\hat{k}\cdot\hat{n})_{PT}\sqrt{n2Plus}+n_{box}\right)\xi_{p\zeta}\right)-\left((\hat{k}\cdot\hat{n})\sqrt{n2Plus}-(\hat{k}\cdot\hat{n})_{PT}n_{box}\right)\\
&\left((\hat{k}\cdot\hat{n})_{PT}\sqrt{n2Minus_{pm}}(\hat{\zeta}\cdot\hat{k})_{pm}\xi_{mnpm}+\left(-(\hat{k}\cdot\hat{n})_{pm}(\hat{k}\cdot\hat{n})_{PT}\sqrt{n2Minus_{pm}}+n_{box}\right)\right.\\
&\left.\xi_{m\zeta pm}\right)\xi_{p\eta}\Big)\Big/\left(NormP\left(-\left((\hat{k}\cdot\hat{n})_{pm}\sqrt{n2Minus_{pm}}-(\hat{k}\cdot\hat{n})_{PT}n_{box}\right)\xi_{m\eta pm}((\hat{k}\cdot\hat{n})_{PT}\right.\right.\\
&\sqrt{n2Plus_{pp}}(\hat{\zeta}\cdot\hat{k})_{pp}\xi_{pnpp}+\left(-(\hat{k}\cdot\hat{n})_{pp}(\hat{k}\cdot\hat{n})_{PT}\sqrt{n2Plus_{pp}}+n_{box}\right)\xi_{p\zeta pp}+\\
&\left((\hat{k}\cdot\hat{n})_{pp}\sqrt{n2Plus_{pp}}-(\hat{k}\cdot\hat{n})_{PT}n_{box}\right)\left((\hat{k}\cdot\hat{n})_{PT}\sqrt{n2Minus_{pm}}(\hat{\zeta}\cdot\hat{k})_{pm}\xi_{mnpm}+\right.\\
&\left.\left.\left.\left(-(\hat{k}\cdot\hat{n})_{pm}(\hat{k}\cdot\hat{n})_{PT}\sqrt{n2Minus_{pm}}+n_{box}\right)\xi_{m\zeta pm}\right)\xi_{p\eta pp}\right)\right)
\end{aligned}
\tag{174}
$$

$$
\begin{aligned}
&r_{--} = -\left(\left(NormM_{mm}\left(-\left((\hat{k}\cdot\hat{n})\sqrt{n2Minus}-(\hat{k}\cdot\hat{n})_{TM}n_{box}\right)\xi_{m\eta}\left((\hat{k}\cdot\hat{n})_{TM}\sqrt{n2Plus_{mp}}\right.\right.\right.\\
&(\hat{\zeta}\cdot\hat{k})_{mp}\xi_{pnmp}+\left(-(\hat{k}\cdot\hat{n})_{mp}(\hat{k}\cdot\hat{n})_{TM}\sqrt{n2Plus_{mp}}+n_{box}\right)\xi_{p\zeta mp}\Big)+\\
&\left((\hat{k}\cdot\hat{n})_{mp}\sqrt{n2Plus_{mp}}-(\hat{k}\cdot\hat{n})_{TM}n_{box}\right)\left((\hat{k}\cdot\hat{n})_{TM}(\hat{\zeta}\cdot\hat{k})\sqrt{n2Minus}\xi_{mn}+\right.\\
&\left.\left.\left(-(\hat{k}\cdot\hat{n})_{TM}(\hat{k}\cdot\hat{n})\sqrt{n2Minus}+n_{box}\right)\xi_{m\zeta}\right)\xi_{p\eta mp}\right)\Big)\Big/\\
&\left(NormM\left(-\left((\hat{k}\cdot\hat{n})_{mm}\sqrt{n2Minus_{mm}}-(\hat{k}\cdot\hat{n})_{TM}n_{box}\right)\xi_{m\eta mm}\left((\hat{k}\cdot\hat{n})_{TM}\sqrt{n2Plus_{mp}}\right.\right.\right.\\
&(\hat{\zeta}\cdot\hat{k})_{mp}\xi_{pnmp}+\left(-(\hat{k}\cdot\hat{n})_{mp}(\hat{k}\cdot\hat{n})_{TM}\sqrt{n2Plus_{mp}}+n_{box}\right)\xi_{p\zeta mp}\Big)+\\
&\left((\hat{k}\cdot\hat{n})_{mp}\sqrt{n2Plus_{mp}}-(\hat{k}\cdot\hat{n})_{TM}n_{box}\right)\left((\hat{k}\cdot\hat{n})_{TM}\sqrt{n2Minus_{mm}}(\hat{\zeta}\cdot\hat{k})_{mm}\xi_{mnmm}+\right.\\
&\left.\left.\left.\left(-(\hat{k}\cdot\hat{n})_{mm}(\hat{k}\cdot\hat{n})_{TM}\sqrt{n2Minus_{mm}}+n_{box}\right)\xi_{m\zeta mm}\right)\xi_{p\eta mp}\right)\right)\Big)
\end{aligned}
\tag{175}
$$

$$
\begin{aligned}
r_{+-} = (&NormM_{pm}\left(\left((\hat{k}\cdot\hat{n})\sqrt{n2Plus}-(\hat{k}\cdot\hat{n})_{PT}n_{box}\right)\left((\hat{k}\cdot\hat{n})_{PT}(\hat{\zeta}\cdot\hat{k})_{pp}\sqrt{n2Plus_{pp}}\xi_{pnpp}+\right.\right.\\
&\left.\left(-(\hat{k}\cdot\hat{n})_{pp}(\hat{k}\cdot\hat{n})_{PT}\sqrt{n2Plus_{pp}}+n_{box}\right)\xi_{p\zeta pp}\right)\xi_{p\eta}-\left((\hat{k}\cdot\hat{n})_{pp}\sqrt{n2Plus_{pp}}-(\hat{k}\cdot\hat{n})_{PT}n_{box}\right)\\
&\left.\left((\hat{k}\cdot\hat{n})_{PT}(\hat{\zeta}\cdot\hat{k})\xi_{pn}\sqrt{n2Plus}+\left(-(\hat{k}\cdot\hat{n})_{PT}(\hat{k}\cdot\hat{n})\sqrt{n2Plus}+n_{box}\right)\xi_{p\zeta}\right)\xi_{p\eta pp}\right)\Big/\\
&\left(NormP\left(\left(-(\hat{k}\cdot\hat{n})_{pm}\sqrt{n2Minus_{pm}}+(\hat{k}\cdot\hat{n})_{PT}n_{box}\right)\xi_{m\eta pm}((\hat{k}\cdot\hat{n})_{PT}(\hat{\zeta}\cdot\hat{k})_{pp}\right.\right.\\
&\sqrt{n2Plus_{pp}}\xi_{pnpp}+\left(-(\hat{k}\cdot\hat{n})_{pp}(\hat{k}\cdot\hat{n})_{PT}\sqrt{n2Plus_{pp}}+n_{box}\right)\xi_{p\zeta pp}\Big)+\\
&\left((\hat{k}\cdot\hat{n})_{pp}\sqrt{n2Plus_{pp}}-(\hat{k}\cdot\hat{n})_{PT}n_{box}\right)\left((\hat{k}\cdot\hat{n})_{PT}(\hat{\zeta}\cdot\hat{k})_{pm}\sqrt{n2Minus_{pm}}\xi_{mnpm}+\right.\\
&\left.\left.\left(-(\hat{k}\cdot\hat{n})_{pm}(\hat{k}\cdot\hat{n})_{PT}\sqrt{n2Minus_{pm}}+n_{box}\right)\xi_{m\zeta pm}\right)\xi_{p\eta pp}\right)\Big)
\end{aligned}
\tag{176}
$$

$$
\begin{aligned}
r_{-+} = &\\
&\left(NormP_{mp}\left(\left(-(\hat{k}\cdot\hat{n})\sqrt{n2Minus}+(\hat{k}\cdot\hat{n})_{TM}n_{box}\right)\left((\hat{k}\cdot\hat{n})_{TM}\sqrt{n2Minus_{mm}}\right.\right.\right.\\
&(\hat{\zeta}\cdot\hat{k})_{mm}\xi_{mnmm}\left(-(\hat{k}\cdot\hat{n})_{mm}(\hat{k}\cdot\hat{n})_{TM}\sqrt{n2Minus_{mm}}+n_{box}\right)\xi_{m\zeta mm}\Big)\xi_{m\eta}+\\
&\left((\hat{k}\cdot\hat{n})_{mm}\sqrt{n2Minus_{mm}}-(\hat{k}\cdot\hat{n})_{TM}n_{box}\right)\left((\hat{k}\cdot\hat{n})_{TM}\sqrt{n2Minus}(\hat{\zeta}\cdot\hat{k})\xi_{mn}+\right.\\
&\left.\left.\left(-(\hat{k}\cdot\hat{n})_{TM}(\hat{k}\cdot\hat{n})\sqrt{n2Minus}+n_{box}\right)\xi_{m\zeta}\right)\xi_{m\eta mm}\right)\Big/\\
&\left(NormM\left(-\left((\hat{k}\cdot\hat{n})_{mm}\sqrt{n2Minus_{mm}}-(\hat{k}\cdot\hat{n})_{TM}n_{box}\right)\xi_{m\eta mm}\left((\hat{k}\cdot\hat{n})_{TM}\sqrt{n2Plus_{mp}}\right.\right.\right.\\
&(\hat{\zeta}\cdot\hat{k})_{mp}\xi_{pnmp}+\left(-(\hat{k}\cdot\hat{n})_{mp}(\hat{k}\cdot\hat{n})_{TM}\sqrt{n2Plus_{mp}}+n_{box}\right)\xi_{p\zeta mp})+\\
&\left((\hat{k}\cdot\hat{n})_{mp}\sqrt{n2Plus_{mp}}-(\hat{k}\cdot\hat{n})_{TM}n_{box}\right)\left((\hat{k}\cdot\hat{n})_{TM}\sqrt{n2Minus_{mm}}(\hat{\zeta}\cdot\hat{k})_{mm}\xi_{mnmm}+\right.\\
&\left.\left.\left(-(\hat{k}\cdot\hat{n})_{mm}(\hat{k}\cdot\hat{n})_{TM}\sqrt{n2Minus_{mm}}+n_{box}\right)\xi_{m\zeta mm}\right)\xi_{p\eta mp}\right)\Big)
\end{aligned}
\tag{177}
$$

$$
\begin{aligned}
tpte = &\left(NormPTE\left(\left((\hat{k}\cdot\hat{n})\sqrt{n2Plus}-(\hat{k}\cdot\hat{n})_{pp}\sqrt{n2Plus_{pp}}\right)\right.\right.\\
&\left(-(\hat{k}\cdot\hat{n})_{PT}(\hat{\zeta}\cdot\hat{k})_{pm}\sqrt{n2Minus_{pm}}\xi_{mnpm}+(\hat{k}\cdot\hat{n})_{pm}(\hat{k}\cdot\hat{n})_{PT}\sqrt{n2Minuspm}\xi_{m\zeta pm}-\right.\\
&\left.n_{box}\xi_{m\zeta pm}\right)\xi_{p\eta}\xi_{p\eta pp}+\xi_{m\eta pm}\left(\left((\hat{k}\cdot\hat{n})_{pm}\sqrt{n2Minus_{pm}}-(\hat{k}\cdot\hat{n})\sqrt{n2Plus}\right)\right.\\
&\left(-(\hat{k}\cdot\hat{n})_{PT}(\hat{\zeta}\cdot\hat{k})_{pp}\sqrt{n2Plus_{pp}}\xi_{pnpp}+(\hat{k}\cdot\hat{n})_{pp}(\hat{k}\cdot\hat{n})_{PT}\sqrt{n2Plus_{pp}}\xi_{p\zeta pp}-n_{box}\xi_{p\zeta pp}\right)\xi_{p\eta}\\
&-\left((\hat{k}\cdot\hat{n})_{pm}\sqrt{n2Minus_{pm}}-(\hat{k}\cdot\hat{n})_{pp}\sqrt{n2Plus_{pp}}\right)\\
&\left.\left.\left(-(\hat{k}\cdot\hat{n})_{PT}(\hat{\zeta}\cdot\hat{k})\sqrt{n2Plus}\xi_{pn}+(\hat{k}\cdot\hat{n})_{PT}(\hat{k}\cdot\hat{n})\sqrt{n2Plus}\xi_{p\zeta}-n_{box}\xi_{p\zeta}\right)\xi_{p\eta pp}\right)\right)/\\
&\left(EPTENormP\left(\left((\hat{k}\cdot\hat{n})_{pm}\sqrt{n2Minus_{pm}}-(\hat{k}\cdot\hat{n})_{PT}n_{box}\right)\xi_{m\eta pm}\right.\right.\\
&\left(-(\hat{k}\cdot\hat{n})_{PT}(\hat{\zeta}\cdot\hat{k})_{pp}\sqrt{n2Plus_{pp}}\xi_{pnpp}+(\hat{k}\cdot\hat{n})_{pp}(\hat{k}\cdot\hat{n})_{PT}\sqrt{n2Plus_{pp}}\xi_{p\zeta pp}-n_{box}\xi_{p\zeta pp}\right)\\
&-\left((\hat{k}\cdot\hat{n})_{pp}\sqrt{n2Plus_{pp}}-(\hat{k}\cdot\hat{n})_{PT}n_{box}\right)\left(-(\hat{k}\cdot\hat{n})_{PT}(\hat{\zeta}\cdot\hat{k})_{pm}\sqrt{n2Minus_{pm}}\xi_{mnpm}+\right.\\
&\left.\left.(\hat{k}\cdot\hat{n})_{pm}(\hat{k}\cdot\hat{n})_{PT}\sqrt{n2Minus_{pm}}\xi_{m\zeta pm}-n_{box}\xi_{m\zeta pm}\right)\xi_{p\eta pp}\right)\Big)
\end{aligned}
\tag{178}
$$

$$
\begin{aligned}
tptm = &\Big(NormP_{TM}\left(\left((\hat{k}\cdot\hat{n})_{pm}\sqrt{n2Minus_{pm}} - (\hat{k}\cdot\hat{n})_{PT}n_{box}\right)\xi_{m\eta pm}\left(-(\hat{\zeta}\cdot\hat{k})\sqrt{n2Plus}\right.\right.\\
&\xi_{pn}\xi_{p\zeta pp} + \xi_{p\zeta}\left((\hat{k}\cdot\hat{n})\sqrt{n2Plus}\xi_{p\zeta pp} + \sqrt{n2Plus_{pp}}\left((\hat{\zeta}\cdot\hat{k})_{pp}\xi_{pnpp} - (\hat{k}\cdot\hat{n})_{pp}\xi_{p\zeta pp}\right)\right)\Big) +\\
&\left((\hat{k}\cdot\hat{n})\sqrt{n2Plus} - (\hat{k}\cdot\hat{n})_{PT}n_{box}\right)\left((\hat{\zeta}\cdot\hat{k})_{pm}\sqrt{n2Minus_{pm}}\xi_{mnpm}\xi_{p\zeta pp} - \xi_{m\zeta pm}\right.\\
&\left.\left((\hat{k}\cdot\hat{n})_{pm}\sqrt{n2Minus_{pm}}\xi_{p\zeta pp} + \sqrt{n2Plus_{pp}}\left((\hat{\zeta}\cdot\hat{k})_{pp}\xi_{pnpp} - (\hat{k}\cdot\hat{n})_{pp}\xi_{p\zeta pp}\right)\right)\right)\xi_{p\eta} +\\
&\left((\hat{k}\cdot\hat{n})_{pp}\sqrt{n2Plus_{pp}} - (\hat{k}\cdot\hat{n})_{PT}n_{box}\right)\left(-(\hat{\zeta}\cdot\hat{k})_{pm}\sqrt{n2Minus_{pm}}\xi_{mnpm}\xi_{p\zeta} + \xi_{m\zeta pm}\right.\\
&\left.\left((\hat{k}\cdot\hat{n})_{pm}\sqrt{n2Minus_{pm}}\xi_{p\zeta} + \sqrt{n2Plus}\left((\hat{\zeta}\cdot\hat{k})\quad(\hat{\zeta}\cdot\hat{k})\xi_{pn} - (\hat{k}\cdot\hat{n})(\hat{k}\cdot\hat{n})\xi_{p\zeta}\right)\right)\xi_{p\eta pp}\right)\Big) /\\
&\Big(EPTMNormP\left(-\left((\hat{k}\cdot\hat{n})_{pm}\sqrt{n2Minuspm} - (\hat{k}\cdot\hat{n})_{PT}n_{box}\right)\xi_{m\eta pm}\right.\\
&\left((\hat{k}\cdot\hat{n})_{PT}(\hat{\zeta}\cdot\hat{k})_{pp}\sqrt{n2Plus_{pp}}\xi_{pnpp} + \left(-(\hat{k}\cdot\hat{n})_{pp}(\hat{k}\cdot\hat{n})_{PT}\sqrt{n2Plus_{pp}} + n_{box}\right)\xi_{p\zeta pp}\right) +\\
&\left((\hat{k}\cdot\hat{n})_{pp}\sqrt{n2Plus_{pp}} - (\hat{k}\cdot\hat{n})_{PT}n_{box}\right)\left((\hat{k}\cdot\hat{n})_{PT}(\hat{\zeta}\cdot\hat{k})_{pm}\sqrt{n2Minus_{pm}}\xi_{mnpm} +\right.\\
&\left.\left.\left(-(\hat{k}\cdot\hat{n})_{pm}(\hat{k}\cdot\hat{n})_{PT}\sqrt{n2Minus_{pm}} + n_{box}n_{box}\right)\xi_{m\zeta pm}\right)\xi_{p\eta pp}\right)\Big)
\end{aligned}
\tag{179}
$$

$$
\begin{aligned}
tmte = &\left(NormM_{TE}\left(\left((\hat{k}\cdot\hat{n})_{mm}\sqrt{n2Minus_{mm}} - (\hat{k}\cdot\hat{n})_{mp}\sqrt{n2Plus_{mp}}\right)\right.\right. \\
&\left(\left(\hat{k}\cdot\hat{n}\right)_{TM}(\hat{\zeta}\cdot\hat{k})\sqrt{n2Minus}\xi_{mn} + \left(-(\hat{k}\cdot\hat{n})_{TM}(\hat{k}\cdot\hat{n})\sqrt{n2Minus} + n_{box}\right)\xi_{m\zeta}\right)\xi_{m\eta mm} \\
&\xi_{p\eta mp} + \xi_{m\eta}\left(\left((\hat{k}\cdot\hat{n})\sqrt{n2Minus} - (\hat{k}\cdot\hat{n})_{mm}\sqrt{n2Minus_{mm}}\right)\xi_{m\eta mm}\left((\hat{k}\cdot\hat{n})_{TM}\sqrt{n2Plus_{mp}}\right.\right. \\
&\left.(\hat{\zeta}\cdot\hat{k})_{mp}\xi_{pnmp} + \left(-(\hat{k}\cdot\hat{n})_{mp}(\hat{k}\cdot\hat{n})_{TM}\sqrt{n2Plus_{mp}} + n_{box}\right)\xi_{p\zeta mp}\right) - \\
&\left(\left(\hat{k}\cdot\hat{n}\right)\sqrt{n2Minus} - (\hat{k}\cdot\hat{n})_{mp}\sqrt{n2Plus_{mp}}\right)\left((\hat{k}\cdot\hat{n})_{TM}\sqrt{n2Minus_{mm}}\right. \\
&\left.\left.\left.(\hat{\zeta}\cdot\hat{k})_{mm}\xi_{mnmm} + \left(-(\hat{k}\cdot\hat{n})_{mm}(\hat{k}\cdot\hat{n})_{TM}\sqrt{n2Minus_{mm}} + n_{box}\right)\xi_{m\zeta mm})\xi_{p\eta mp}\right)\right)\right) / \\
&\left(EMTENormM\left(-\left((\hat{k}\cdot\hat{n})_{mm}\sqrt{n2Minus_{mm}} - (\hat{k}\cdot\hat{n})_{TM}n_{box}\right)\xi_{m\eta mm}\left((\hat{k}\cdot\hat{n})_{TM}\right.\right.\right. \\
&\sqrt{n2Plus_{mp}}(\hat{\zeta}\cdot\hat{k})_{mp}\xi_{pnmp} + \left(-(\hat{k}\cdot\hat{n})_{mp}(\hat{k}\cdot\hat{n})_{TM}\sqrt{n2Plus_{mp}} + n_{box}\right)\xi_{p\zeta mp}\Big) + \\
&\left((\hat{k}\cdot\hat{n})_{mp}\sqrt{n2Plus_{mp}} - (\hat{k}\cdot\hat{n})_{TM}n_{box}\right)\left((\hat{k}\cdot\hat{n})_{TM}\sqrt{n2Minus_{mm}}(\hat{\zeta}\cdot\hat{k})_{mm}\xi_{mnmm} + \right. \\
&\left.\left.\left.\left(-(\hat{k}\cdot\hat{n})_{mm}(\hat{k}\cdot\hat{n})_{TM}\sqrt{n2Minus_{mm}} + n_{box}\right)\xi_{m\zeta mm}\right)\xi_{p\eta mp}\right)\right)
\end{aligned}
\tag{180}
$$

$$
\begin{aligned}
tmtm = &\Big(NormM_{TM}\left(\left(\sqrt{n2Minus_{mm}}\left((\hat{k}\cdot\hat{n})\sqrt{n2Minus}-(\hat{k}\cdot\hat{n})_{TM}n_{box}\right)\right.\right.\\
&(\hat{\zeta}\cdot\hat{k})_{mm}\xi_{mnmm}\xi_{m\eta}+\sqrt{n2Minus}(\hat{\zeta}\cdot\hat{k})\left(-(\hat{k}\cdot\hat{n})_{mm}\sqrt{n2Minus_{mm}}+(\hat{k}\cdot\hat{n})_{TM}n_{box}\right)\\
&\left.\xi_{mn}\xi_{m\eta mm}\right)\xi_{p\zeta mp}+\xi_{m\zeta}\left(\left((\hat{k}\cdot\hat{n})_{mm}\sqrt{n2Minus_{mm}}-(\hat{k}\cdot\hat{n})_{TM}n_{box}\right)\xi_{m\eta mm}\right.\\
&\left((\hat{k}\cdot\hat{n})\sqrt{n2Minus}\xi_{p\zeta mp}+\sqrt{n2Plus_{mp}}\left((\hat{\zeta}\cdot\hat{k})_{mp}\xi_{pnmp}-(\hat{k}\cdot\hat{n})_{mp}\xi_{p\zeta mp}\right)\right)+\\
&\sqrt{n2Minus_{mm}}\left(-(\hat{k}\cdot\hat{n})_{mp}\sqrt{n2Plusmp}+(\hat{k}\cdot\hat{n})_{TM}n_{box}\right)(\hat{\zeta}\cdot\hat{k})_{mm}\xi_{mnmm}\xi_{p\eta mp}\Big)+\\
&\xi_{m\zeta mm}\left(-\left((\hat{k}\cdot\hat{n})\sqrt{n2Minus}-(\hat{k}\cdot\hat{n})_{TM}n_{box}\right)\xi_{m\eta}\right.\\
&\left((\hat{k}\cdot\hat{n})_{mm}\sqrt{n2Minus_{mm}}\xi_{p\zeta mp}+\sqrt{n2Plus_{mp}}\left((\hat{\zeta}\cdot\hat{k})_{mp}\xi_{pnmp}-(\hat{k}\cdot\hat{n})_{mp}\xi_{p\zeta mp}\right)\right)+\\
&\left((\hat{k}\cdot\hat{n})_{mp}\sqrt{n2Plus_{mp}}-(\hat{k}\cdot\hat{n})_{TM}n_{box}\right)\left((\hat{\zeta}\cdot\hat{k})\xi_{mn}\sqrt{n2Minus}+\right.\\
&\left.\left.\left.\left(-(\hat{k}\cdot\hat{n})\sqrt{n2Minus}+(\hat{k}\cdot\hat{n})_{mm}\sqrt{n2Minus_{mm}}\right)\xi_{m\zeta}\right)\xi_{p\eta mp}\right)\right)\Big)\Big/\\
&(EMTMNormM\left(-\left((\hat{k}\cdot\hat{n})_{mm}\sqrt{n2Minus_{mm}}-(\hat{k}\cdot\hat{n})_{TM}n_{box}\right)\xi_{m\eta mm}\left((\hat{k}\cdot\hat{n})_{TM}\right.\right.\\
&\sqrt{n2Plus_{mp}}(\hat{\zeta}\cdot\hat{k})_{mp}\xi_{pnmp}+\left(-(\hat{k}\cdot\hat{n})_{mp}(\hat{k}\cdot\hat{n})_{TM}\sqrt{n2Plus_{mp}}+n_{box}\right)\xi_{p\zeta mp}\Big)+\\
&\left((\hat{k}\cdot\hat{n})_{mp}\sqrt{n2Plus_{mp}}-(\hat{k}\cdot\hat{n})_{TM}n_{box}\right)((\hat{k}\cdot\hat{n})_{TM}\sqrt{n2Minus_{mm}}(\hat{\zeta}\cdot\hat{k})_{mm}\xi_{mnmm}+\\
&\left.\left.\left(-(\hat{k}\cdot\hat{n})_{mm}(\hat{k}\cdot\hat{n})_{TM}\sqrt{n2Minus_{mm}}+n_{box}\right)\xi_{m\zeta mm})\xi_{p\eta mp}\right)\right)
\end{aligned}
\tag{181}
$$

VITA

B.S. in Physics, 2012 - Southeastern Louisiana University